Human Molecular Genetics, 2006, Vol. 15, No. 8 *1279–1289*
doi:10.1093/hmg/ddl045
Advance Access published on March 10, 2006

Aberrant neuromuscular junctions and delayed terminal muscle fiber maturation in α-dystroglycanopathies

Mariko Taniguchi[1], Hiroki Kurahashi[3], Satoru Noguchi[4], Takayasu Fukudome[5], Takeshi Okinaga[2], Toshifumi Tsukahara[6], Youichi Tajima[7], Keiichi Ozono[2], Ichizo Nishino[4], Ikuya Nonaka[4] and Tatsushi Toda[1,*]

[1]Division of Clinical Genetics, Department of Medical Genetics and [2]Department of Pediatrics, Osaka University Graduate School of Medicine, 2-2 Yamadaoka, Suita, Osaka 565-0871, Japan, [3]Division of Molecular Genetics, Institute for Comprehensive Medical Science, Fujita Health University, Toyoake, Aichi 470-1192, Japan, [4]National Institute of Neuroscience, National Center of Neurology and Psychiatry, Kodaira, Tokyo 187-8502, Japan, [5]Division of Clinical Research, Nagasaki Medical Center of Neurology, Kawatanamachi, Nagasaki 859-3615, Japan, [6]Center for Nano Materials and Technology, Japan Advanced Institute of Science and Technology, Tatsunokuchi, Ishikawa 923-1292, Japan and [7]Department of Clinical Genetics, The Tokyo Metropolitan Institute of Medical Science, Bunkyo-ku, Tokyo 113-8613, Japan

Received October 15, 2005; Revised and Accepted February 28, 2006

Recent studies have revealed an association between post-translational modification of α-dystroglycan (α-DG) and certain congenital muscular dystrophies known as secondary α-dystroglycanopathies (α-DGpathies). Fukuyama-type congenital muscular dystrophy (FCMD) is classified as a secondary α-DGpathy because the responsible gene, *fukutin*, is a putative glycosyltransferase for α-DG. To investigate the pathophysiology of secondary α-DGpathies, we profiled gene expression in skeletal muscle from FCMD patients. cDNA microarray analysis and quantitative real-time polymerase chain reaction showed that expression of developmentally regulated genes, including myosin heavy chain (*MYH*) and myogenic transcription factors (*MRF4*, *myogenin* and *MyoD*), in FCMD muscle fibers is inconsistent with dystrophy and active muscle regeneration, instead more of implicating maturational arrest. FCMD skeletal muscle contained mainly immature type 2C fibers positive for immature-type MYH. These characteristics are distinct from Duchenne muscular dystrophy, suggesting that another mechanism in addition to dystrophy accounts for the FCMD skeletal muscle lesion. Immunohistochemical analysis revealed morphologically aberrant neuromuscular junctions (NMJs) lacking MRF4 co-localization. Hypoglycosylated α-DG indicated a lack of aggregation, and acetylcholine receptor (AChR) clustering was compromised in FCMD and the myodystrophy mouse, another model of secondary α-DGpathy. Electron microscopy showed aberrant NMJs and neural terminals, as well as myotubes with maturational defects. Functional analysis of NMJs of α-DGpathy showed decreased miniature endplate potential and higher sensitivities to *d*-Tubocurarine, suggesting aberrant or collapsed formation of NMJs. Because α-DG aggregation and subsequent clustering of AChR are crucial for NMJ formation, hypoglycosylation of α-DG results in aberrant NMJ formation and delayed muscle terminal maturation in secondary α-DGpathies. Although severe necrotic degeneration or wasting of skeletal muscle fibers is the main cause of congenital muscular dystrophies, maturational delay of muscle fibers also underlies the etiology of secondary α-DGpathies.

*To whom correspondence should be addressed. Tel: +81 668793380; Fax: +81 668793389; Email: toda@clgene.med.osaka-u.ac.jp

INTRODUCTION

Fukuyama-type congenital muscular dystrophy (FCMD; MIM 253800) is an autosomal recessive muscular dystrophy and the second most common childhood muscular dystrophy in Japan, following Duchenne muscular dystrophy (DMD) (1). Clinical manifestations of FCMD include severe congenital muscular dystrophy from early infancy, cobblestone lissencephaly and eye malformation. We previously isolated the responsible gene for FCMD, termed *fukutin* (2,3). Recently, it has been postulated that *fukutin* modulates the glycosylation of α-dystroglycan (α-DG), a major component of the dystrophin–glycoprotein complex (4,5). FCMD is classified as one of the congenital muscular dystrophies, such as laminin-α2-deficient congenital muscular dystrophy (MDC1A) (6). Recently, FCMD has also been classified as a secondary α-DGpathy, as mutations in genes encoding glycosyltransferases result in hypoglycosylated α-DG (7). α-Dystroglycan binds to extracellular matrix proteins such as laminin, agrin and perlecan, which are important in maintaining muscle cell integrity (8). Hypoglycosylated α-DG provokes the post-translational disruption of dystroglycan–ligand interactions in the skeletal muscle of patients, leading to the severe phenotypes of congenital muscular dystrophies (7). Other glycosyltransferases include POMGnT1 (protein *O*-mannose β-1, 2-*N*-acetylglucosaminyltransferase 1), POMT1 and POMT2 (protein *O*-mannosyltransferases 1 and 2), fukutin-related protein (FKRP) and LARGE; mutations in these genes induce human muscle–eye–brain disease, Walker–Warburg syndrome and congenital muscular dystrophy type 1C/1D, and mouse myodystrophy, respectively (9–14).

Primary characteristics of the so-called 'muscular dystrophy' such as DMD include necrotic change and active regeneration of muscle fibers. From infancy, DMD patients usually show dystrophic change in skeletal muscle, accompanied by elevation of serum creatine kinase (CK) levels. However, DMD patients usually maintain their gait until early adolescence. In contrast, FCMD patients show severe phenotypic characteristics from very early infancy, and few patients can acquire gait regardless of serum CK levels (1). Skeletal muscle fibers in FCMD are extremely small, irregular in cell size and architecturally disorganized, and extensive fibrosis prevails from the early infantile stage. However, only a small number of muscle fibers show severe necrotic change or active myofibril regeneration, and satellite cells are also fewer than those of DMD (1,15,16). These phenotypic differences promote the hypothesis that another mechanism may also account for the pathophysiology of secondary α-DGpathies.

Although expression profiling of skeletal muscle from patients with DMD, MDC1A and α-sarcoglycanopathy have been described (17–19), no similar analysis has been reported for FCMD and other secondary α-DGpathies. To investigate the molecular mechanism of FCMD and other secondary α-DGpathies, we profiled gene expression in FCMD skeletal muscle using cDNA microarray and subsequent quantitative real-time polymerase chain reaction (PCR). Here we demonstrate that aberrant neuromuscular junctions (NMJs) and maturational delay of muscle fibers are significant to the mechanism underlying secondary α-DGpathies.

RESULTS

Aberrant muscle regeneration is suggested by gene expression profiling of FCMD skeletal muscle

Gene expression profiling of FCMD skeletal muscle was performed using a custom cDNA microarray. Clustering analysis showed similar overall expression profiles of muscle from four FCMD patients, aged 20 days to 1 year, 6 months (Fig. 1A). This similarity is independent of age and histology of the muscle specimen in our samples.

We analyzed individual genes showing distinct expression patterns in FCMD skeletal muscle compared with normal children or DMD patients. Most genes encoding muscle components were down-regulated in FCMD. Among these, *myosin light chain 1, 3* and *4* (*myl1, 3* and *4*) were up-regulated in DMD skeletal muscle, in contrast with FCMD (Fig. 1B). Expression of the developmentally regulated myosin heavy chains (*MYHs*), *MYH1*, *MYH2* and *MYH7* (slow, adult-type), was down-regulated in FCMD but not in DMD, whereas expression of *MYH8* (fast-type) showed no significant change in FCMD compared with DMD or normal controls. Slow-type MYHs (MYH1, MYH2 and MYH7) are present in mature muscle fibers and crucial for sarcomere assembly to maintain muscle integrity, whereas fast-type or developmental MYHs (MYH3, MYH4 and MYH8) are seen in early immature myoblasts or in regenerating fibers. These observations suggest that expression of mature muscle components is suppressed in FCMD skeletal muscle at all ages examined.

With regard to muscle fiber differentiation, myogenic factors including *MyoD*, *myf5* and *myogenin* (*myf4*) showed insufficient signal for the analysis. It is noteworthy, however, that *MRF4* (*myf6*) was down-regulated in FCMD. Expression of the alpha-type cholinergic receptor (*CHRNA*), which is known to be regulated by *MyoD* and *MRF4* (20,21), was much higher in FCMD patients than in normal controls.

We next performed real-time quantitative PCR to further investigate skeletal muscle differentiation. We compared mRNA expression in FCMD muscle with normal or DMD skeletal muscle, as DMD is a good example for active regeneration, in which expression of muscle component and myogenic factor mRNA expression is expected to be up-regulated. Although *CHNRA* was up-regulated in DMD, as predicted, its expression was even higher in FCMD (Fig. 2A and B). Among these cholinergic receptor subtypes, gamma-type cholinergic receptor (*CHNRG*), which is a component of fetal isoforms, was up-regulated, whereas epsilon-type cholinergic receptor (*CHNRE*), which only composes adult isoforms (22), was down-regulated in FCMD (Fig. 2B). MYH slow-type (*MYH7*) was down-regulated in FCMD, consistent with the microarray analysis, whereas expression of fast-type MYH (*MYH11b*) was not altered in FCMD. Interestingly, although *MyoD* and *myogenin* were up-regulated in both DMD and FCMD, *MRF4* was down-regulated in FCMD muscle but up-regulated in DMD (Fig. 2A and B). *MRF4* expression is known to be up-regulated in the late phase of muscle regeneration or differentiation, followed by sequential expression of *MyoD*, *myf5* and *myogenin*, indicating significant roles in terminal differentiation (20,21). These results suggest that FCMD skeletal muscle undergoes an unbalanced differentiation process.

A

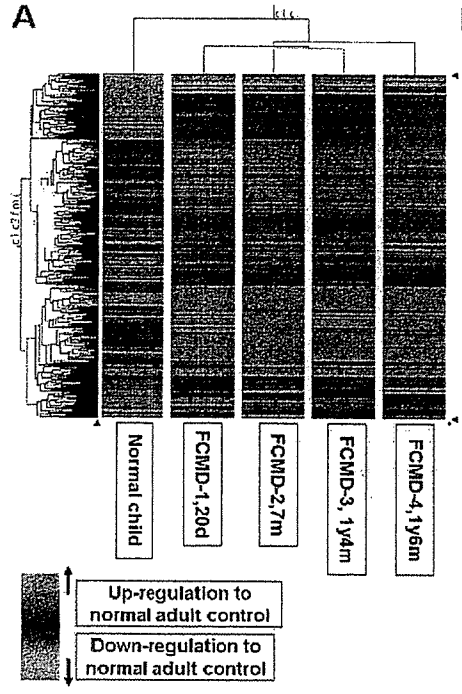

B

gene	FCMD	DMD	Product
myl1	↓	→	myosin light chain 1
myl2	↓	↑	myosin light chain 2
myl3	↓	↑	myosin light chain 3
myl4	↓	↑	atrial /embryonic alkali myosin light chain
myh1	↓↓	↑	myosin, heavy polypeptide 1, adult (slow)
myh2	↓↓	↑	myosin, heavy polypeptide 2, adult (slow)
myh7	↓↓	↑	myosin, heavy polypeptide 7, beta (slow)
myh8	↓	→	myosin, heavy polypeptide 8, (fast)
mybpc1	↓↓	↑	myosin binding protein C, slow type
mybph	↑	→	myosin-binding protein H
actc	↑	↑	actin, alpha, cardiac muscle precursor
actg1	↓	↑	actin, gamma 1
actg2	↓	↑↑	actin, gamma 2
sgcb	↓↓	↓	sarcoglycan, beta
tcap	↓↓	→	titin-cap (telethonin)
ttn	↓↓	↓	titin
des	↓↓	↑	desmin
myf6	↓	→	MRF4 (myf6,herculin)
CHRNA	↑↑	→	nicotinic type, acetylcholine receptor

Figure 1. Cluster image and gene trees from expression profiling of FCMD and normal skeletal muscle. (**A**) Each line corresponds to the expression signal of each gene. Genes are ordered using the average linkage clustering method to group similar expression profiles. Red denotes up-regulated genes and green denotes down-regulated genes compared with adult control muscle. Note that the expression trends are almost identical within FCMD patients, and FCMD trends are distinct from those of normal children. (B) Expression profile of major muscle components of FCMD and DMD compared with that of normal children. Arrows show the relative expression change (single upward arrow and downward arrow, more than 2-fold increase/decrease; double upward arrows and downward arrows, more than 10-fold increase/decrease; rightward arrow, no change). Note that majority of muscle components are down-regulated in FCMD muscles.

Final maturation step is retarded in FCMD skeletal muscle

To investigate how differentiation is impaired, we examined histological specimens of FCMD skeletal muscle. Marked interstitial tissues with numerous small, round-shaped immature fibers and some necrotic fibers increased with age were seen in FCMD skeletal muscle specimens. Interstitial tissue is prominent from early infancy and progresses with age (Fig. 3A–C), and skeletal muscle from an FCMD fetus also shows rich interstitial tissues (Fig. 3E). Although necrotic change in muscle fibers is not so marked as in DMD fibers, DMD muscle shows less marked fibrosis and more mature fibers, despite more active necrotic and regenerating processes (Fig. 3D). Overall, FCMD muscle is reminiscent of fetal muscle; skeletal muscle from a normal fetus appears rich in fibrous tissues and small, round-shaped immature myotubes (Fig. 3F).

Muscle fiber type is easily identified by ATPase staining. Normally, type 2C fibers are mainly seen in fetal muscle fibers or in regenerating fibers. However, in ATPase-stained cryospecimens, FCMD muscle showed a significantly higher percentage of undifferentiated type 2C muscle fiber contents relative to DMD or control samples ($P < 0.005$) (Fig. 3G and H, Table 1).

Using immunohistochemical analysis, we examined MYH subtypes to confirm the differentiation impairment in FCMD and in myodystrophy mouse (*myd*), which is another model of secondary α-DGpathies. In normal muscle from age-matched controls, no staining of developmental or neonatal MYH (Fig. 3I and J) was seen. In contrast, FCMD and *myd* muscle fibers stained positively for developmental and neonatal MYHs (Fig. 3M and N). These positive fibers corresponded with those staining positive for fast-type MYHs in a serial section (Fig. 3M–O, arrows). Similar staining patterns were observed in skeletal muscle from an FCMD fetus. It is unlikely that all fibers showing developmental MYH expression are derived from regenerating fibers, as few active regenerating or necrotic fibers are seen in the hematoxylin and eosin (HE) specimen at any ages (Fig. 3A–C). Similar staining patterns were observed in skeletal muscles from an FCMD fetus and adult *myd* (data not shown). It is unlikely that all fibers showing developmental MYH expression are derived from regenerating fibers, as few active regenerating or necrotic fibers are seen in the HE specimen (Fig. 3A–C).

These results induce the possibility that maturation might be slowed or arrested in FCMD and *myd* skeletal muscles, and possibly this is common in secondary α-DGpathies. It also

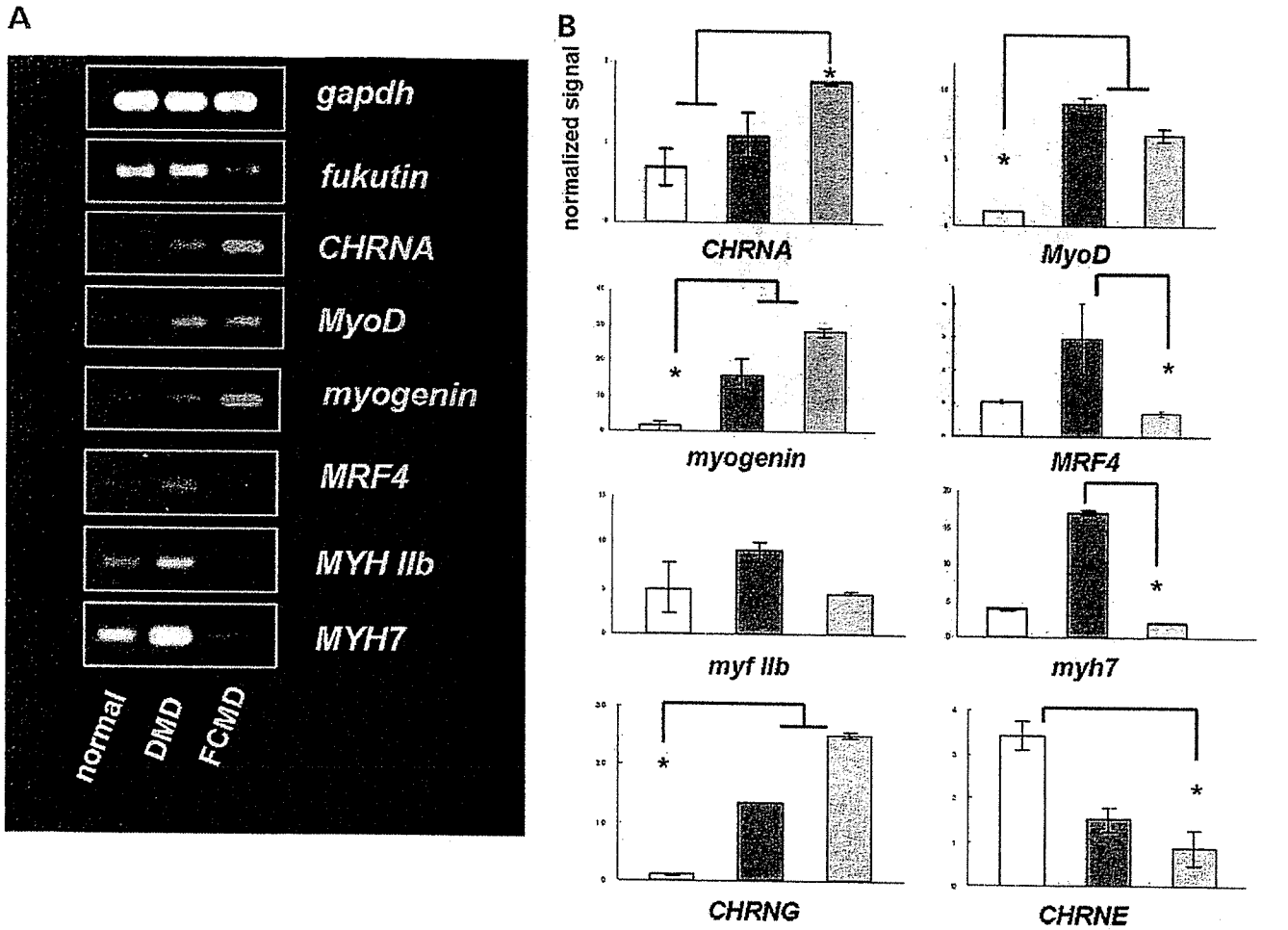

Figure 2. Differential expression of muscle components and myogenic factors in skeletal muscles from FCMD, DMD and normal children. (**A**) PCR products show that *MyoD* and *myogenin*, which are sequentially expressed in the early phase of muscle regeneration, are up-regulated in DMD and FCMD; however *MYH* and *MRF4* are down-regulated in FCMD but not DMD. (**B**) Quantitative real-time PCR analysis of mRNA expression. Each bar represents the mean value and 95% confidence interval of duplicate experiments in two patients for each disease and normal control. White bar, normal children; black bar, DMD; gray bar, FCMD. Expression levels are plotted as values normalized to *gapdh*. $^*P < 0.005$ (Student's *t*-test).

implies that secondary α-DGpathies have more complex etiology than the so-called 'muscular dystrophy', and that may be partly explained by a maturational defect.

NMJ abnormalities induce maturational delay in secondary α-DGpathies

Microarray analysis showed a reduction in *MRF4* expression in FCMD. Using immunochemistry, we further investigated MRF4 expression in FCMD and in *myd*. Immunoreactivity against MRF4 was reduced dramatically in FCMD muscle fibers (Fig. 4A). In normal skeletal muscles, anti-MRF4 antibody yielded strong signals, which co-localized with the nucleus and NMJs (Fig. 4A, upper columns). MRF4 in FCMD muscles showed weak signals which were not merged with NMJ (Fig. 4A, lower columns). Similar results were obtained in *myd* (data not shown). Regarding the fact that MRF4 is required at the time and place of NMJ development during skeletal muscle differentiation (23), these results prompt the hypothesis that the differentiation process of muscle fibers arrests at this point in secondary α-DGpathies.

We next examined the morphology of NMJs in both FCMD and *myd* by staining acetylcholine receptor (AchR) in NMJs with anti-α-bungarotoxin (Fig. 4B). Almost all the NMJs of FCMD and *myd* showed sparse, weak staining (Fig. 4B, lower columns), in contrast with the dense pattern in normal skeletal muscle (Fig. 4B, upper columns). In normal skeletal muscles, the borders of positive signals were characteristically flared because of multiple layers of synaptic folds, whereas borders in FCMD and *myd* appear smooth and simple, and synaptic folds—particularly secondary folds—were seldom observed. This signal pattern reflects deteriorated or non-deteriorated cluster of AChR on NMJs in secondary α-DGpathies.

Electron microscopic examination of these secondary α-DGpathies revealed aberrant NMJ lesions with abnormal neural endings. NMJs with fewer synaptic folds and secondary clefts were seen in all NMJs of FCMD and *myd* (Fig. 5A–F). In addition, the muscle fibers showed characteristics of immaturity, consistent with our hypothesis that the myotubes are maturationally arrested (Fig. 5G and H). These fibers are distinct from the active regenerating

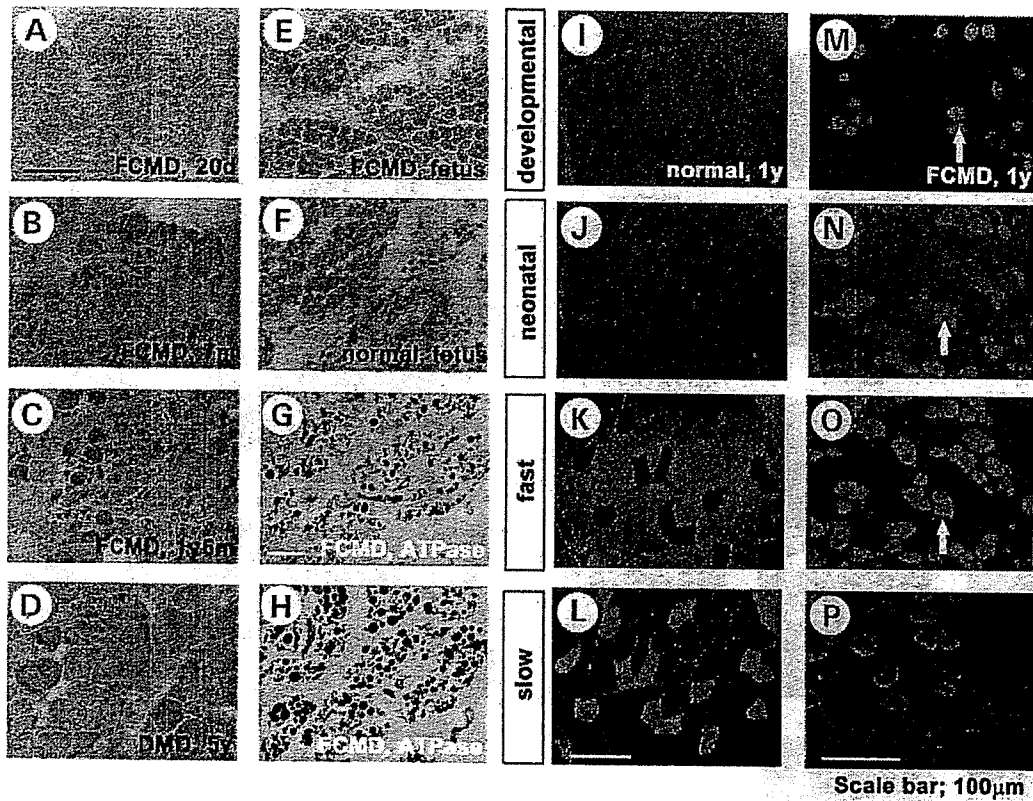

Figure 3. HE and ATPase stains of biopsied FCMD skeletal muscle, used for microarray analysis. Each specimen shows marked fibrosis with numerous small immature muscle fibers, which is seen from early infancy (**A**, 20 days; **B**, 7 months; **C**, 1-year 6 months), and progresses with age. DMD muscle (**D**, 5 years) shows less marked fibrosis and less frequent immature fibers despite more active necrotic and regenerating processes. Note that the pathological findings of FCMD skeletal muscles are similar to those of fetal skeletal muscles (**E**, FCMD fetus, 19 weeks; **F**, normal fetus, 21 weeks). Also note many undifferentiated immature type 2C fibers stained darkly for ATPase under both alkaline (pH 10.4) (**G**) and acid (pH 4.6) (**H**) pre-incubations. Immunostaining for MYH subtypes shows positive staining of developmental and neonatal MYH and decreased staining of slow-type MYH, which are distinct from normal muscles (normal child muscles, 1 year, **I**–**L**; FCMD, 1 year, **M**–**P** in sequential cryosections). Scale bars = 100 μm.

Table 1. Muscle contents and type 2C fibers in biopsied specimen of FCMD, DMD and normal children

Disease	Age	Muscle (%)	Type 2C (%)	Fibrosis (%)
FCMD (F1)	20 days	71	26	27
FCMD (F2)	7 months	53	26	41
FCMD (F3)	1-year 4 months	60	25	42
FCMD (F4)	1-year 6 months	52	19	43
DMD[a]	3–9 years	61	9	30
Normal[a]	1 year	>95	<5	<5

[a]Average, $n = 10$.

myotubes seen in DMD muscle fibers, in that ribosome particles appear quite poor.

We performed functional analysis of the morphologically aberrant NMJs in secondary α-DGpathy by measuring miniature endplate potential (MEPP) and endplate potential (EPP) of *myd* mice (Table 2). The amplitudes of MEPP were markedly lower in *myd* mice than in normal littermates ($P < 0.005$). In contrast, quantal content of EPP was increased in *myd* ($P < 0.005$). The reduction of MEPP amplitude could be compensated by the increased quantal content, and the safety margin of neuromuscular transmission is considered to be maintained in *myd* mice. The number of endplates recorded in *myd* mice was much fewer than in normal littermates. However, the amount of *d*-Tubocurarine that can inhibit the muscle contraction induced by the EPP was distinctively low for *myd* muscle relative to that of normal littermate (Table 2). These findings implicate, combined with the morphological observation, that most of the endplates in *myd* are not adequately innervated, but a small number of NMJs functionally compensate the low MEPP amplitude to maintain the safety margin of neuromuscular transmission.

Hypoglycosylation of α-DG as the etiology of non-clustering AChR in NMJs

We performed immunostaining to examine core α-DG in muscle fibers. In normal skeletal muscles, α-DG localized to the NMJ and sarcoplasmic membrane (Fig. 6A). In contrast, FCMD and *myd* showed substantial α-DG on the sarcoplasmic membrane, but only weak signals were observed in thin NMJs, indicating a failure of α-DG aggregation (Fig. 6A, normal NMJs, arrows; FCMD and *myd*, arrowheads). We also examined staining of glycosylated α-DG (IIH6). As expected, we saw no signal on NMJs or on the sarcoplasmic membrane in FCMD and *myd* (data not shown), implying that glycosylation

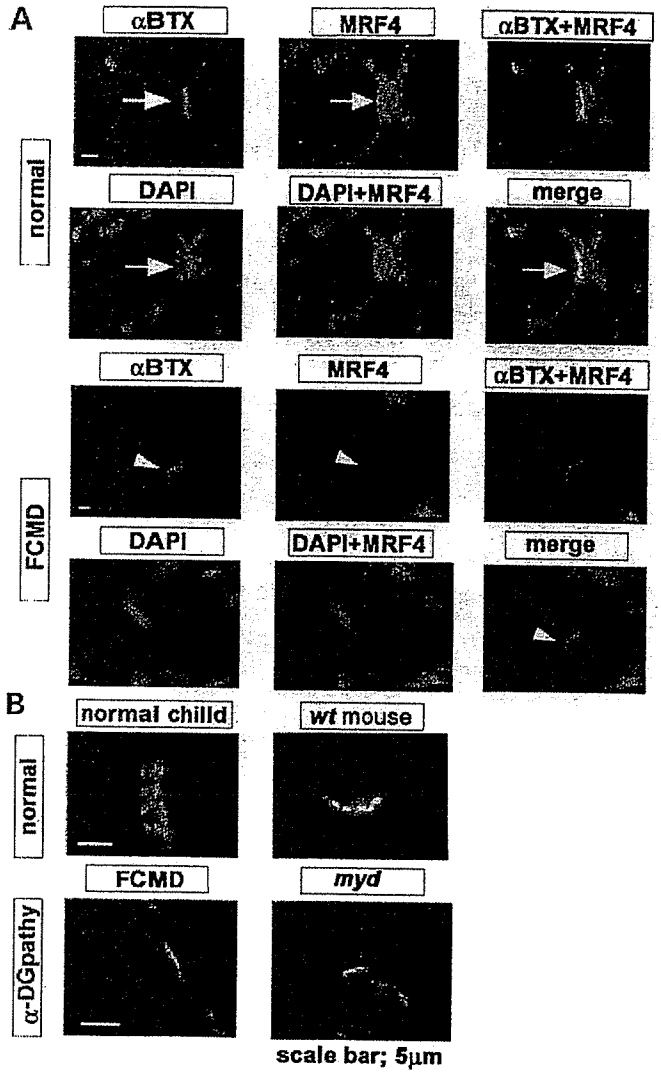

Figure 4. Immunohistochemistry of MRF4 in secondary α-DGpathy and aberrant NMJs in secondary α-DGpathy. (A) Fluorescence image of MRF4 (green), α-bungarotoxin staining of AChR on NMJ (red) and DAPI-stained nuclei (blue) in normal and FCMD skeletal muscles. In normal muscle, NMJs stain strongly, merging with MRF4 staining and DAPI (arrows, upper columns). In FCMD, the staining pattern of MRF4 in the nucleus of muscle fibers is markedly decreased and no merging stain with NMJ is seen (arrowhead). (B) Compared with normal AChR on NMJs (red) stained by α-BTX (upper columns), scattered, fold-less staining pattern is present in both FCMD and *myd* (lower columns). Scale bars = 5 μm.

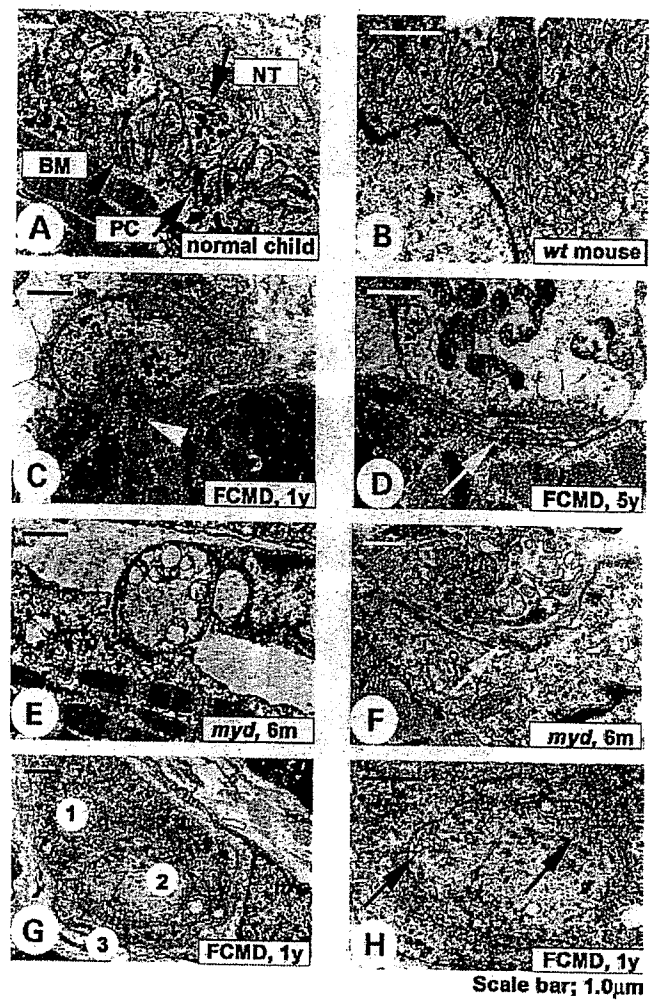

Figure 5. Electron microscopic examinations of NMJs and skeletal muscle from secondary α-DGpathies. Aberrant NMJs and myotubes with maturational arrest are seen in secondary α-DGpathies. Compared with normal (A, human; B, *wt* mouse), NMJs in FCMD (C and D) and *myd* (E and F) show simpler secondary clefts and wider synaptic clefts with occasional multilayered basal lamina (D and F, white arrows). Moreover, maturationally arrested myotubes are seen in secondary α-DGpathy. Three cells (1–3) share a common basement membrane (G), and at higher magnification, these myotubes contain poorly organized myofibrils (black arrows) (H). In contrast with early regenerating fibers in normal regenerating myotubes, ribosome particles are not abundant in FCMD, indicating maturational arrest of myotubes in secondary α-DGpathy. Abbreviation: PC, primary cleft; NT, nerve terminal; BM, basal lamina. Scale bars = 1.0 μm.

is crucial for α-DG aggregation and also for the subsequent clustering of AChR in NMJs. α-DG is expressed on both the muscle peripheral membrane and the peripheral nerve terminal at NMJs (24). Thus, we examined whether a pre-synaptic or post-synaptic lesion contributes to aberrant NMJ formation. Staining for synaptophysin at the pre-synaptic region or for fasciculin at the synaptic gap showed abnormal patterns similar to that of α-bungarotoxin (Fig. 6B). These observations indicate that NMJ abnormalities in secondary α-DGpathies may arise not only at the post-synaptic muscle peripheral membrane, but also by pre-synaptic hypoglycosylated α-DG.

Utrophin and dystrophin are expressed abundantly in pre- and post-synaptic regions of mature NMJs and suggested to play an important role for synaptic maturation and the maintenance of NMJs (25). To analyze aberrations of the distribution of utrophin and dystrophin, we performed immunostaining for utrophin and dystrophin in NMJs. Examination under confocal microscopy allowed a precise view of both proteins on the sarcoplasmic membrane. In NMJs from a normal sample, utrophin strongly stains exclusively at fine primary and secondary synaptic folds, tangled with dystrophin staining just beneath the muscle peripheral membrane (Fig. 6C, left column; Fig. 6D, upper columns). In contrast, NMJs from secondary α-DGpathies show thinner, fold-less and weak signals for both utrophin and dystrophin (Fig. 6C, right column; Fig. 6D, middle and lower

Table 2. Functional analysis of NMJs in *myd* mice

	MEPP amplitude (mV)[a]	Quantal content (m)[a]	*d*-Tubocurarine concentration (μg/ml)[b]
Control 1	0.52 ± 0.07 ($n = 16$)	49.1 ± 5.5 ($n = 10$)	0.38
Control 2	0.64 ± 0.10 ($n = 18$)	52.8 ± 3.8 ($n = 14$)	0.45
myd 1	0.32 ± 0.04 ($n = 11$)	65.6 ± 6.5 ($n = 5$)	0.30
myd 2	0.36 ± 0.06 ($n = 7$)	75.4 ± 38.7 ($n = 5$)	0.30

[a]Values given are mean ± SEM and number of endplates (in parentheses).
[b]The amount of *d*-Tubocurarine that can inhibit the muscle contraction induced by the EPP.

columns). The utrophin signal was exclusively seen on NMJs, but weakly seen on muscle sarcoplasmic membrane in FCMD (Fig. 6C, right column), which is usually seen in regenerating muscle fibers (26). NMJs from fetal wild-type or *myd* showed similar staining patterns as expected (data not shown), suggesting that this staining pattern is indicative of immature muscle fibers. This observation is consistent with our hypothesis that NMJ formation in secondary α-DGpathies is developmentally arrested during myotube maturation in the fetal phase.

DISCUSSION

FCMD has long been classified as 'muscular dystrophy', although the clinical characteristics differ from those of DMD. Muscular dystrophy is defined generally by necrotic change and active regeneration of muscle fibers. However, FCMD muscle in infantile stage seems more likely to have additional features, implying a more complex pathogenesis for FCMD. Indeed, our microarray analysis showed that general expression profiling clusters FCMD and DMD distinctively. Expression of mature muscle components was surprisingly low in FCMD, indicating less active regeneration of muscle fibers. We also saw similar expression profiles among all FCMD patients in our samples, indicating that FCMD is a chronic rather than progressive disorder, at least at the infantile period.

We confirmed maturational delay and aberrant NMJs in FCMD skeletal muscle fibers by expression profiling, morphological and histochemical analysis, and electrophysiological examination. These findings are common to secondary α-DGpathies but are not seen in DMD. In this study, we demonstrate that the etiology of secondary α-DGpathy skeletal muscle abnormalities may stem from maturational arrest caused by aberrant NMJs in addition to dystrophy. MDC1A, clinical characteristics of which are similar to FCMD, is described with an initial phase of necrosis and regeneration in the early steps of the disease (6). Although aberrant NMJ is also seen in MDC1A (27), the muscle fragility due to defect in the component of basement membrane mainly affects the phenotype and causes necrosis and regeneration.

A considerable body of evidence indicates that muscle differentiation ceases at NMJ formation in FCMD. First, immature type 2C fibers are predominant in FCMD (Table 1). At the initiation of muscle differentiation, satellite cells proliferate to become myoblasts, fuse to organize myotubes. These early myotubes contain type 2C fibers. Following NMJ formation, immature fibers are induced to differentiate further into mature muscle fibers such as type 1, 2A and 2B. Second, down-regulated expression of matured MYHs in FCMD also suggests arrest at this stage. Following completion of NMJ formation, embryonic, neonatal-type MYHs in immature myofibers are replaced by adult-type, slow MYHs, which are induced by extracellular matrix (ECM) components, growth factors or programmed cell differentiation (28).

Third, MRF4, which is postulated to be induced by AChR clustering in NMJ formation, is down-regulated in FCMD. Normally, during the early phase of muscle development, a series of myogenic regulatory genes such as *myf5*, *MyoD* and *myogenin* are sequentially expressed; followed by MRF4 up-regulation just after NMJ formation. AChRs bind to myotubes, associate with specific factors and trigger a signal to induce expression of myogenic factors including MRF4, which is suggested to play a crucial role in muscle terminal maturation and maintenance (20,21,29). Therefore, MRF4 is distinct from MyoD, myogenin and myf5 in that it is expressed mainly in matured myotubes and myofibers. MRF4 has been reported to co-localize with AChR in NMJs and to function in terminal muscle maturation and fiber maintenance (30). It is reasonable to assume that MRF4 function is required at the time and place of NMJ development during skeletal muscle differentiation (23). These results prompt the hypothesis that the differentiation process of muscle fibers arrests at this point in FCMD and *myd*.

Fourth, the fact that high *CHRNG* and low *CHRNE* expression in FCMD muscle relative to that in age-matched normal control or DMD muscle is striking, although the age of the DMD patient was slightly higher than that of the FCMD patients. It clearly indicates that most of the AChR in FCMD muscle is fetal type. It also supports our hypothesis that skeletal muscle in secondary α-DGpathy is immature and that delay of differentiation might be involved with maturation defect of NMJs.

What causes aberrant NMJs in secondary α-DGpathies? Normally, NMJs are built by a dense tangle of sarcoplasmic membrane and neural endings through a layer of basement membrane. It is possible that connections between the neural terminal and glycosylated α-DG, made through a layer of basement membrane and mediated by molecules such as laminin or agrin, are important to normal NMJ formation and subsequent muscle differentiation (31,32). MDC1A, clinical characteristics of which are similar to FCMD (6), also shows aberrant NMJs with fewer synaptic folds (27). In contrast, Musk or rapsyn deficiency does not resemble severe muscular dystrophy in spite of the abnormal NMJ formation. The interaction of laminin and α-DG is thought to play an essential role in the transition of AChR microaggregates into macroaggregates at the developing NMJ, followed by the concentration of α-DG on NMJs (32,33). These facts lend support to our hypothesis that the laminin/α-DG interaction fulfills a pivotal function in normal NMJ formation.

Alternatively, it is also possible that attachment of neural terminals to NMJs is affected pre-synaptically in secondary α-DGpathies. Abnormalities in the pre-synaptic peripheral nerve would affect the neural endings of NMJs, leading to

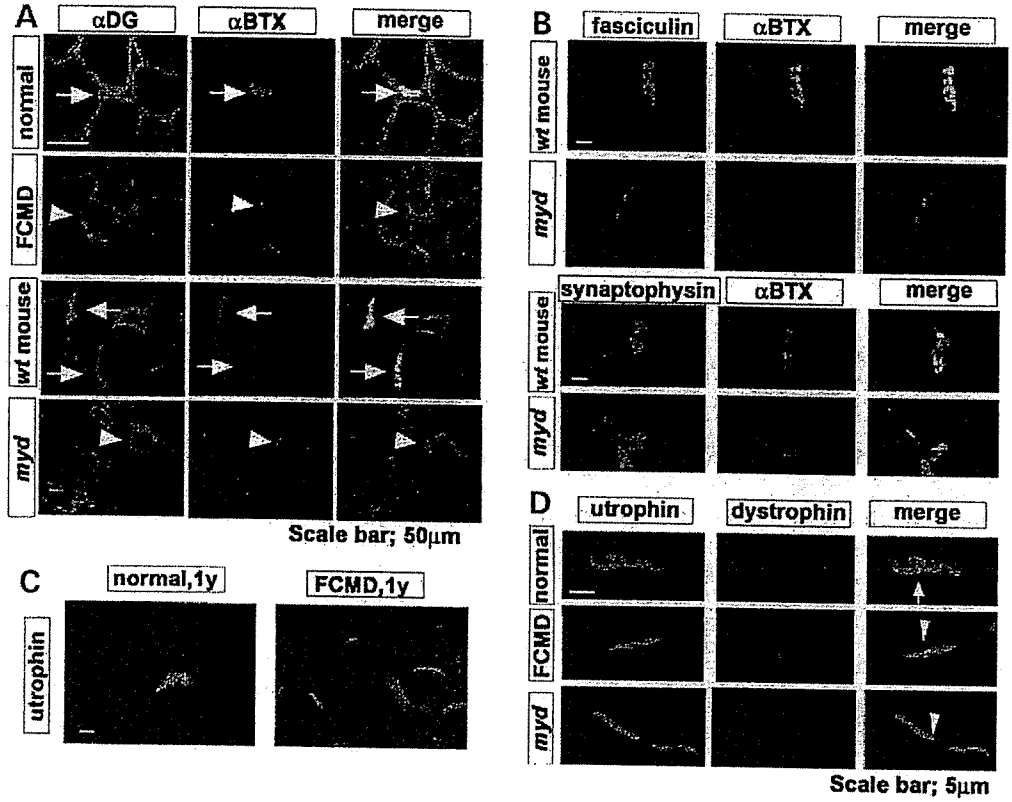

Figure 6. Aberrant NMJs and lack of α-dystroglycan aggregation in NMJs affect pre- and post-synaptic formation of NMJs in secondary α-DGpathy. (**A**) α-DG (green) strongly co-localizes with α-BTX in NMJs of normal skeletal muscle, merged yellow (arrows). However in secondary α-DGpathies, the lack of α-dystroglycan aggregation on aberrant formed NMJs is seen despite positive staining on muscle peripheral membrane, as evidenced by the lack of co-localization signal in merged columns (arrowheads). (**B**) Green-stained pre-synaptic markers (fasciculin, AChE marker; synaptophysin, pre-synaptic vesicle marker) also show the aberrant staining pattern of NMJs, shown in merged staining with α-BTX (red) in *myd*. (**C**) Utrophin remains on sarcoplasmic membrane on secondary α-DGpathies. Although green-stained utrophin aggregates exclusively on NMJs of normal muscle fibers, utrophin remains on sarcoplasmic membrane of FCMD muscle fibers. (**D**) Confocal imaging of utrophin and dystrophin on NMJs of secondary α-DGpathy. Merged column in normal NMJs (arrow) shows that fine primary and secondary folds lined with utrophin are tangled with dystrophin staining on NMJs, which also line the peripheral membrane of muscle fibers. Note that in secondary α-DGpathies, secondary folds are severely lacking (arrowheads). Thin, scattered utrophin staining and markedly decreased staining of dystrophin on NMJs are seen in both FCMD and *myd*. Scale bars = 5 μm.

deficient differentiation signal transduction to FCMD muscle fibers and arrested post-synaptic muscle differentiation. It has been suggested that α-DG in the central or peripheral nervous system is hypoglycosylated in secondary α-DGpathies (34). *O*-Mannose-type glycoprotein is suggested to contribute to the stability and maintenance of muscle cell membrane, synaptic formation and myelination of peripheral nerves, although the precise mechanism of α-DG activity in peripheral nerve tissue is unclear. The dystrophin–glycoprotein complex on Schwann cells is also thought to be important in peripheral myelinogenesis, regeneration, differentiation, apoptosis and polarity of skeletal muscle cells (35). Although Ishii *et al.* (36) reported that electron microscopy of Schwann cells on FCMD muscle revealed no pathologic findings, neural transmission may be developmentally impaired and collapsed as a result of hypoglycosylated α-DG.

Naturally, our data do not rule out the other possibilities for immaturity of the skeletal muscles of α-DGpathies. Although the expression profile and histochemical data indicate that skeletal muscles are in a persistent undifferentiated state, it is possible that the regeneration process fulfills a crucial function in the phenomenon observed in skeletal muscles of α-DGpathies. It is also possible that most of the muscle fibers are under denervation status, because motor neurons are unable to maintain strong attachments to myofibers, leading to a constant stimulation of denervation signal pathways. Although we demonstrated substantial evidences for the aberrant NMJ, the pathogenesis of skeletal muscles in α-DGpathies is likely to be a combination of these problems and of multifactorial origin.

Taken together, these findings show that muscle fibers in secondary α-DGpathies are developmentally arrested more to 'dystrophic', perhaps because hypoglycosylated α-DG precludes proper aggregation on NMJs, preventing AChR clustering. These defects may disrupt terminal muscle maturation, which is induced after innervation of neurons on the muscle peripheral membrane via a basement membrane layer. Dystrophic changes traditionally thought to underlie 'muscular dystrophy' are caused by attenuated physical connections between α-DG and the muscle basement membrane. We propose that the muscle lesion in secondary α-DGpathies is caused by complex pathogenesis, not only by dystrophic change but more importantly, maturational arrest resulting from chronically delayed terminal muscle fiber maturation and NMJ deficiency. To date, no clinical approaches to secondary α-DGpathies exist. These findings open a possible

avenue for treating muscle tissues in these congenital muscular dystrophies, via targeted induction of NMJ maturation in muscle fibers.

MATERIALS AND METHODS

Samples

All clinical materials were collected for diagnostic purposes. Four muscle specimens (biceps branchii) from FCMD patients (ages: 20 days, 7 months, 1-year 4 months, and 1-year 6 months) were used in the analysis. Genetic screening identified a homozygous retrotransposal insertion into the 3′ untranslated region of *fukutin* in all FCMD patients (3). For the non-dystrophic muscle controls, muscle RNAs from two children (ages: 1 year) was used. These patients were selected based on normal laboratory findings, normal plasma CK levels and no histopathological evidence for muscular dystrophy.

We also obtained myodystrophy ($Large^{myd}$) mice and control littermates ($Large^{myd/+}$ or $Large^{+/+}$), aged 3 and 6 months, by mating heterozygous pairs provided by Jackson Laboratories.

RNA isolation and expression profiling

Generation of cDNA microarrays containing skeletal muscle transcripts has been reported previously (19). Using similar methods, we constructed a new cDNA chip containing 5600 genes expressed in skeletal muscle. RNA isolation, hybridization and detection methods also have been reported previously. Microarray experiments were carried out using a competitive hybridization method with two labeled targets: one for muscle RNAs from FCMD patients or normal children, and another for pooled muscle RNAs (Origene), which served as a template control for per-chip normalization. Each analysis was conducted at least twice. The hybridization intensities of each spot and the background intensities were calculated using a ScanArray 5000 microarray scanner with Quant Array software (Perkin-Elmer Life Science).

Microarray data analysis

Analysis of microarray data was performed using Genespring version 6.1 (Silicon Genetics) software. Data used for further analysis were calculated using a previously reported method (19). To avoid 'false-positive' signals, we excluded genes from the analysis for which average normal expression level constraints are under 500. We sorted 1790 genes from a total of 5600 for further analysis.

Quantitative real-time PCR

Two patients with FCMD (ages: 10 months and 1 year), two patients with DMD (ages: 1 and 7 years) and two normal children (ages: 1 and 2 years) were used for quantitative RT–PCR using skeletal muscle RNAs. Single-strand cDNA was produced with random primers, and quantitative real-time RT–PCR using SYBR-green was performed using the ABI Prism 7900 sequence detection system (Applied Biosynthesis). Data analysis was performed in duplicate experiments. Statistical significance was evaluated using Student's *t*-test, and $P < 0.05$ was considered significant. The primers used for the experiments are shown in Supplementary Material, Table S1. *Gapdh* was used as an internal control.

Imaging analysis

HE staining and ATPase staining were performed on cryosections. ATPase staining was performed at pH 9.4–10.6 and 4.2–4.6. For ATPase staining, average data from 10 DMD patients (ages: 3–9) and 10 normal control cases (ages: around 1 year) were selected. Scion Image Beta 3b (Scion Corporation) was used for estimating the content of type 2C fibers, muscle fibers, adipose tissues and interstitial tissues (Table 1). Statistical analysis was performed using Student's *t*-test.

Immunohistochemistry

All muscle specimens were processed for cryosectioning (8-μm thick) and fixed in 50% ethanol and 50% acetic acid for 1 min. Anti-core α-dystroglycan [GT20ADG, gift from Dr Kevin Campbell (5)], rhodamine-conjugated α-bungarotoxin (BTX, Molecular Probes), anti-synaptophysin (NCL-SYNAPp, Novocastra), Alexa-fluor488 labeled anti-fasciculin2 (F4293, Sigma), anti-MRF4 (C-19, Cruz Biotechnology), anti-utrophin (UT2, gift from Dr Michihiro Imamura), anti-human dystrophin (NCL-DYS2, Novocastra), anti-human dystrophin (MANDRA-1, Sigma) and anti-myosin heavy chain for developmental, neonatal, fast and slow types (NCL-MHCd, MHCn, MHCf and MHCs, respectively, Novocastra) were used to stain NMJs.

Electron microscopy

Muscle specimens were obtained from four patients diagnosed as FCMD (ages: 6 months to 4 years old) and from two normal children (ages: 1 year). Five NMJs were found in three FCMD patients' skeletal muscle and four normal NMJs were examined in two normal children. Intercostal muscles and soleus muscles were dissected from myodystrophy and control mice, and cut into 1-mm thick cubes. Four NMJs were examined in myd and normal controls, respectively. Samples were fixed in 2% glutaraldehyde and embedded in epoxy resin as described previously (36). Ultrathin (50–90-nm thick) sections were cut on an Ultracut S ultramicrotome (Reichert).

Electrophysiologic examination

Diaphragms with its motor nerve were dissected and used for the conventional intracellular microelectrode study (37). MEPPs, EPPs and resting membrane potentials (RMPs) were recorded. For EPP recording, the phrenic nerve was stimulated using a suction electrode at 0.5 Hz. *d*-Tubocurarine chloride (Curaren, Sigma) was used at a concentration sufficient to inhibit muscle contraction. The potentials were corrected for non-linear summation and the last 64 responses in a train of 114 were saved for later analysis. The quantal content *m* was calculated by the variance method. MEPP and EPP amplitudes were corrected to a standard RMP of −80 mV. To correct MEPP amplitude by the fiber diameter, the geometric

mean of the shortest and longest diameters of muscle fibers was determined in 30 randomly selected muscle fibers in cryostat sections.

SUPPLEMENTARY MATERIAL

Supplementary Material is available at HMG Online.

ACKNOWLEDGEMENTS

We are grateful to Drs Fumiaki Saito and Shin'ichi Takeda for their critical comments, Fumie Uematsu and Eiji Oiki for technical support and Dr Jennifer Logan for editing the manuscript. This work was supported by a Health Science Research Grant, Research on Psychiatric and Neurological Diseases and Mental Health, from the Ministry of Health, Labor, and Welfare of Japan; and by the 21st Century COE program from the Ministry of Education, Culture, Sports, Science, and Technology of Japan.

Conflict of Interest statement. None declared.

REFERENCES

1. Fukuyama, Y., Osawa, M. and Suzuki, H. (1981) Congenital progressive muscular dystrophy of the Fukuyama type—clinical, genetic and pathological considerations. *Brain Dev.*, **3**, 1–29.
2. Toda, T., Segawa, M., Nomura, Y., Nonaka, I., Masuda, K., Ishihara, T., Sakai, M., Tomita, I., Origuchi, Y., Suzuki, M. *et al.* (1993) Localization of a gene for Fukuyama type congenital muscular dystrophy to chromosome 9q31–33. *Nat. Genet.*, **5**, 283–286.
3. Kobayashi, K., Nakahori, Y., Miyake, M., Matsumura, K., Kondo-Iida, E., Nomura, Y., Segawa, M., Yoshioka, M., Saito, K., Osawa, M. *et al.* (1998) An ancient retrotransposal insertion causes Fukuyama-type congenital muscular dystrophy. *Nature*, **394**, 388–392.
4. Hayashi, Y.K., Ogawa, M., Tagawa, K., Noguchi, S., Ishihara, T., Nonaka, I. and Arahata, K. (2001) Selective deficiency of alpha-dystroglycan in Fukuyama-type congenital muscular dystrophy. *Neurology*, **57**, 115–121.
5. Michele, D.E., Barresi, R., Kanagawa, M., Saito, F., Cohn, R.D., Satz, J.S., Dollar, J., Nishino, I., Kelley, R.I., Somer, H. *et al.* (2002) Post-translational disruption of dystroglycan–ligand interactions in congenital muscular dystrophies. *Nature*, **418**, 417–422.
6. Tome, F.M., Evangelista, T., Leclerc, A., Sunada, Y., Manole, E., Estournet, B., Barois, A., Campbell, K.P. and Fardeau, M. (1994) Congenital muscular dystrophy with merosin deficiency. *CR Acad. Sci. III.* **317**, 381–357.
7. Muntoni, F., Brockington, M., Blake, D.J., Torelli, S. and Brown, S.C. (2002) Defective glycosylation in muscular dystrophy. *Lancet*, **360**, 1419–1421.
8. Hohenester, E., Tisi, D., Talts, J.F. and Timpl, R. (1999) The crystal structure of a laminin G-like module reveals the molecular basis of alpha-dystroglycan binding to laminins, perlecan, and agrin. *Mol. Cell.*, **4**, 783–792.
9. Yoshida, A., Kobayashi, K., Manya, H., Taniguchi, K., Kano, H., Mizuno, M., Inazu, T., Mitsuhashi, H., Takahashi, S., Takeuchi, M. *et al.* (2001) Muscular dystrophy and neuronal migration disorder caused by mutations in a glycosyltransferase, POMGnT1. *Dev. Cell.*, **1**, 717–724.
10. Beltran-Valero de Bernabe, D., Currier, S., Steinbrecher, A., Celli, J., van Beusekom, E., van der Zwaag, B., Kayserili, H., Merlini, L., Chitayat, D., Dobyns, W.B. *et al.* (2002) Mutations in the *O*-mannosyltransferase gene POMT1 give rise to the severe neuronal migration disorder Walker Warburg syndrome. *Am. J. Hum. Genet.*, **71**, 1033–1043.
11. van Reeuwijk, J., Janssen, M., van den Elzen, C., Beltran-Valero de Bernabe, D., Sabatelli, P., Merlini, L., Boon, M., Scheffer, H., Brockington, M., Muntoni, F. *et al.* (2005) POMT2 mutations cause alpha-dystroglycan hypoglycosylation and Walker Warburg syndrome. *J. Med. Genet.*, **12**, 907–912.
12. Brockington, M., Yuva, Y., Prandini, P., Brown, S.C., Torelli, S., Benson, M.A., Herrmann, R., Anderson, L.V., Bashir, R., Burgunder, J.M. *et al.* (2001) Mutations in the fukutin-related protein gene (FKRP) identify limb girdle muscular dystrophy 2I as a milder allelic variant of congenital muscular dystrophy MDC1C. *Hum. Mol. Genet.*, **10**, 2851–2859.
13. Grewal, P.K., Holzfeind, P.J., Bittner, R.E. and Hewitt, J.E. (2001) Mutant glycosyltransferase and altered glycosylation of alpha-dystroglycan in the myodystrophy mouse. *Nat. Genet.*, **28**, 151–154.
14. Longman, C., Brockington, M., Torelli, S., Jimenez-Mallebrera, C., Kennedy, C., Khalil, N., Feng, L., Saran, R.K., Voit, T., Merlini, L. *et al.* (2003) Mutations in the human LARGE gene cause MDC1D, a novel form of congenital muscular dystrophy with severe mental retardation and abnormal glycosylation of alpha-dystroglycan. *Hum. Mol. Genet.*, **12**, 2853–2861.
15. Nonaka, I., Sugita, H., Takada, K. and Kumagai, K. (1982) Muscle histochemistry in congenital muscular dystrophy with central nervous system involvement. *Muscle Nerve*, **5**, 102–106.
16. Terasawa, K. (1986) Muscle regeneration and satellite cells in Fukuyama type congenital muscular dystrophy. *Muscle Nerve*, **5**, 465–470.
17. Chen, Y.W., Zhao, P., Borup, R. and Hoffman, E.P. (2000) Expression profiling in the muscular dystrophies: identification of novel aspects of molecular pathophysiology. *J. Cell Biol.*, **151**, 1321–1336.
18. Haslett, J.N., Sanoudou, D., Kho, A.T., Bennett, R.R., Greenberg, S.A., Kohane, I.S., Beggs, A.H. and Kunkel, L.M. (2002) Gene expression comparison of biopsies from Duchenne muscular dystrophy (DMD) and normal skeletal muscle. *Proc. Natl Acad. Sci. USA*, **99**, 15000–15005.
19. Noguchi, S., Tsukahara, T., Fujita, M., Kurokawa, R., Tachikawa, M., Toda, T., Tsujimoto, A., Arahata, K. and Nishino, I. (2003) cDNA microarray analysis of individual Duchenne muscular dystrophy patients. *Hum. Mol. Genet.*, **12**, 595–600.
20. Prody, C.A. and Merlie, J.P. (1991) A developmental and tissue-specific enhancer in the mouse skeletal muscle acetylcholine receptor alpha-subunit gene regulated by myogenic factors. *J. Biol. Chem.*, **266**, 22588–22596.
21. Fujisawa-Sehara, A., Nabeshima, Y., Komiya, T., Uetsuki, T., Asakura, A. and Nabeshima, Y. (1992) Differential *trans*-activation of muscle-specific regulatory elements including the myosin light chain box by chicken MyoD, myogenin, and MRF4. *J. Biol. Chem.*, **267**, 10031–10038.
22. Mishina, M., Takai, T., Imoto, K., Noda, M., Takahashi, T., Numa, S., Methfessel, C. and Sakmann, B. (1986) Molecular distinction between fetal and adult forms of muscle acetylcholine receptor *Nature*, **321**, 406–411.
23. Sunyer, T. and Merlie, J.P. (1993) Cell type- and differentiation-dependent expression from the mouse acetylcholine receptor epsilon-subunit promoter. *J. Neurosci. Res.*, **36**, 224–234.
24. Jacinthe, G. and Michael, F. (2001) Expression and localization of agrin during sympathetic synapse formation *in vitro*. *J. Neurobiol.*, **48**, 228–242.
25. Grady, R.M., Zhou, H., Cunningham, J.M., Henry, M.D., Campbell, K.P. and Sanes, J.R. (2000) Maturation and maintenance of the neuromuscular synapse: genetic evidence for roles of the dystrophin–glycoprotein complex. *Neuron*, **25**, 279–293.
26. Helliwell, T.R., Man, N.T., Morris, G.E. and Davies, K.E. (1992) The dystrophin-related protein, utrophin, is expressed on the sarcolemma of regenerating human skeletal muscle fibres in dystrophies and inflammatory myopathies. *Neuromuscul. Disord.*, **3**, 177–184.
27. Noakes, P.G., Gautam, M., Mudd, J., Sanes, J.R. and Merlie, J.P. (1995) Aberrant differentiation of neuromuscular junctions in mice lacking *s*-laminin/laminin beta 2. *Nature*, **374**, 258–262.
28. Miller, J.B. and Stockdale, F.E. (1986) Developmental origins of skeletal muscle fibers: clonal analysis of myogenic cell lineages based on expression of fast and slow myosin heavy chains. *Proc. Natl Acad. Sci. USA*, **83**, 3860–3864.

29. Weis, J., Kaussen, M., Calvo, S. and Buonanno, A. (2000) Denervation induces a rapid nuclear accumulation of MRF4 in mature myofibers. *Dev. Dyn.*, **218**, 438–451.
30. Zhou, Z. and Bornemann, A. (2001) MRF4 protein expression in regenerating rat muscle. *J. Muscle. Res. Cel. Motil.*, **22**, 311–316.
31. Campanelli, J.T., Roberds, S.L., Campbell, K.P. and Scheller, R.H. (1994) A role for dystrophin-associated glycoproteins and utrophin in agrin-induced AChR clustering. *Cell*, **77**, 663–674.
32. Kahl, J. and Campanelli, J.T. (2003) A role for the juxtamembrane domain of beta-dystroglycan in agrin-induced acetylcholine receptor clustering. *J. Neurosci.*, **23**, 392–402.
33. Jacobson, C., Cote, P.D., Rossi, S.G., Rotundo, R.L. and Carbonetto, S. (2001) The dystroglycan complex is necessary for stabilization of acetylcholine receptor clusters at neuromuscular junctions and formation of the synaptic basement membrane. *J. Cell Biol.*, **152**, 435–450.
34. Saito, F., Moore, S.A., Barresi, R., Henry, M.D., Messing, A., Ross-Barta, S.E., Cohn, R.D., Williamson, R.A., Sluka, K.A., Sherman, D.L. *et al.* (2003) Unique role of dystroglycan in peripheral nerve myelination, nodal structure, and sodium channel stabilization. *Neuron*, **38**, 747–758.
35. Leschziner, A., Moukhles, H., Lindenbaum, M., Gee, S.H., Butterworth, J., Campbell, K.P. and Carbonetto, S. (2000) Neural regulation of alpha-dystroglycan biosynthesis and glycosylation in skeletal muscle. *J. Neruochem.*, **74**, 70–80.
36. Ishii, H., Hayashi, Y.K., Nonaka, I. and Arahata, K. (1997) Electron microscopic examination of basal lamina in Fukuyama congenital muscular dystrophy. *Neuromuscul. Disord.*, **7**, 191–197.
37. Nagel, A., Lehmann-Horn, F. and Engel, A.G. (1990) Neuromuscular transmission in the mdx mouse. *Muscle Nerve*, **13**, 742–749.

doi:10.1093/brain/awl077

Brain (2006), 129, 1470–1480

Central core disease is due to *RYR1* mutations in more than 90% of patients

Shiwen Wu,[1] Carlos A. Ibarra M,[1] May Christine V. Malicdan,[1] Kumiko Murayama,[1] Yasuko Ichihara,[2] Hirosato Kikuchi,[3] Ikuya Nonaka,[1] Satoru Noguchi,[1] Yukiko K. Hayashi[1] and Ichizo Nishino[1]

[1]Department of Neuromuscular Research, National Institute of Neuroscience, National Center of Neurology and Psychiatry (NCNP), Kodaira, [2]Department of Anesthesiology, Tokyo Rinkai Hospital, Tokyo and [3]Department of Anesthesiology, Saitama Medical School, Saitama, Japan

Correspondence to: Ichizo Nishino, MD, PhD, Department of Neuromuscular Research, National Institute of Neuroscience, National Center of Neurology and Psychiatry (NCNP), 4-1-1 Ogawahigashi-cho, Kodaira, Tokyo 187-8502, Japan
E-mail: nishino@ncnp.go.jp

Ryanodine receptor 1 (*RYR1*) gene mutations are associated with central core disease (CCD), multiminicore disease (MmD) and malignant hyperthermia (MH), and have been reported to be responsible for 47–67% of patients with CCD and rare cases with MmD. However, to date, the true frequency and distribution of the mutations along the *RYR1* gene have not been determined yet, since mutation screening has been limited to three 'hot spots', with particular attention to the C-terminal region. In this study, 27 unrelated Japanese CCD patients were included. Clinical histories and muscle biopsies were carefully reviewed. We sequenced all the 106 exons encoding RYR1 with their flanking exon–intron boundaries, and identified 20 novel and 3 previously reported heterozygous missense mutations in 25 of the 27 CCD patients (93%), which is a much higher mutation detection rate than that perceived previously. Among them, six were located outside the known 'hot spots'. Sixteen of 27 (59%) CCD patients had mutations in the C-terminal 'hot spot'. Three CCD patients had a probable autosomal recessive disease with two heterozygous mutations. Patients with C-terminal mutations had earlier onset and rather consistent muscle pathology characterized by the presence of distinct cores in almost all type 1 fibres, interstitial fibrosis and type 2 fibre deficiency. In contrast, patients with mutations outside the C-terminal region had milder clinical phenotype and harbour more atypical cores in their muscle fibres. We also sequenced two genes encoding RYR1-associated proteins as candidate causative genes for CCD: the 12 kD FK506-binding protein (*FKBP12*) and the α1 subunit of L-type voltage-dependent calcium channel or dihydropyridine receptor (*CACNA1S*). However, no mutation was found, suggesting that these genes may not, or only rarely, be responsible for CCD. Our results indicate that CCD may be caused by *RYR1* mutations in the majority of patients.

Keywords: central core disease; genotype–phenotype correlation; muscular dystrophy; myopathy; ryanodine receptor 1 mutations

Abbreviations: CACNA1S = α1 subunit of L-type voltage-dependent calcium channel; CCD = central core disease; CICR = calcium-induced calcium release; EC = excitation–contraction; *FKBP12* = FK506-binding protein, 12 kD; mGT = modified Gomori–Trichrome; MmD = multiminicore disease; MH = malignant hyperthermia; *RYR1* = ryanodine receptor 1; SERCA = sarco-endoplasmic reticulum Ca^{2+} ATPase; SR = sarcoplasmic reticulum

Received October 28, 2005. Revised March 1, 2006. Accepted March 8, 2006. Advance Access publication April 18, 2006

Introduction

Central core disease (CCD) was the first described congenital myopathy in humans (Shy and Magee, 1956), usually inherited in an autosomal dominant pattern, except for few reports on autosomal recessive cases (Manzur *et al.*, 1998; Jungbluth *et al.*, 2002). The clinical features are quite variable (Quinlivan *et al.*, 2003), ranging from lack of visible weakness or abnormality to lack of independent ambulation. Most of the patients, in classical descriptions, have a slowly or

non-progressive proximal muscle weakness and hypotonia during infancy that can persist throughout adolescence/adulthood, and have associated delayed motor development and reduced muscle bulk. In addition, musculoskeletal alterations including congenital hip dislocation, kyphoscoliosis and joint contractures are also common findings in CCD patients (Lorenzon *et al.*, 2000; Quinlivan *et al.*, 2003). The diagnosis is commonly made from muscle biopsy by the presence of cores in type 1 fibres, which are typically well demarcated and located centrally in the fibres. A few cores, however, can be located in the subsarcolemmal regions of individual type 1 muscle fibres. Longitudinal sections show that the core runs the whole length of the fibre.

Recent reports have documented that the phenotypic presentation varies considerably from no visible disability to lack of independent ambulation. While the overall incidence of CCD is rare, the absence of symptoms in a significant number of patients may suggest that the actual incidence of CCD may be considerably higher than that perceived currently.

CCD has been linked to the gene encoding the skeletal muscle ryanodine receptor, *RYR1*, and is considered to be an allelic disease of malignant hyperthermia (MH) susceptibility. This is a pharmacogenetic disorder with autosomal dominant inheritance in which susceptible individuals develop generalized muscle contracture followed by a hypermetabolic state due to massive calcium release from the sarcoplasmic reticulum (SR), when they are exposed to inhaled general anaesthetics or to the depolarizing muscle relaxant succinylcholine. CCD patients have higher probability to be susceptible to MH. The *RYR1* mutations linked to MH and CCD are clustered in three relatively restricted regions of the protein or 'hot spots': N-terminal (residues p.M1-R614), central (p.R2163–p.R2458) and C-terminal (p.R4136-p.P4973). They are also called domains 1–3, respectively (Treves *et al.*, 2005). The first two domains are located in the soluble cytoplasmic regions of the protein. Most of the CCD mutations are clustered in domain 3, which is located in the C-terminus and comprises the transmembrane/luminal and pore-forming region of the channel (McCarthy *et al.*, 2000; Monnier *et al.*, 2001; Davis *et al.*, 2003). Hence, mutations in this region of the protein may directly alter the permeation/selectivity/gating properties of the channel (Balshaw *et al.*, 1999).

The *RYR1* is one of the largest described genes in humans, spanning >159 kb in size on chromosome 19.q13.1. A 15 117-nucleotide-long open reading frame encoded in 106 exons (two of which are alternatively spliced) produces a 563 kD protein. In addition, it forms a homotetrameric structure that functions as an SR calcium-release channel regulating Ca^{2+} content in skeletal muscle during excitation–contraction (EC) coupling. Because of the size of the *RYR1* gene, efficient routine screening for mutations has been difficult. Most of the *RYR1* mutation screenings in CCD patients have been limited to the above-mentioned three 'hot spots' or even to the C-terminal region alone, and 47–67% patients were found carrying *RYR1* mutations (Monnier *et al.*, 2001; Davis *et al.*, 2003; Shepherd *et al.*, 2004), which suggested that CCD is a genetically heterogeneous disease. Here, we screened all the exons and flanking exon–intron boundaries of *RYR1* in order to determine the frequency and distribution of mutations, and describe the genotype–phenotype correlation in Japanese patients with CCD.

Although no mutation in other genes has been associated with CCD, many studies have shown that mutants of the RYR1-associated proteins FKBP12 and CACNA1S cause EC uncoupling *in vitro* just as some *RYR1* mutants do (Avila *et al.*, 2003*b*; Lyfenko *et al.*, 2004; Weiss *et al.*, 2004), raising a possibility that *FKBP12* and/or *CACNA1S* mutations may also be responsible for CCD. In addition, the mutations in the *RYR1*-binding domain of *CACNA1S* are thought to account for 1% of MH patients (Stewart *et al.*, 2001). We therefore sequenced the entire open reading frame of *FKBP12* and the part of *CACNA1S* that encodes the *RYR1*-binding region.

Methods

Subjects

Unrelated Japanese CCD patients were selected for the study from the *National Center of Neurology and Psychiatry (NCNP)* database from 1982 to 2004. CCD diagnosis was established on the basis of characteristic muscle pathology findings of cores almost exclusively in type 1 fibres. We excluded multiminicore disease (MmD) cases, which had multiple cores in >70% of type 1 fibres in our series. Available blood samples from the patients' relatives were also included in the analysis. In addition, DNA samples from 150 subjects without any known muscle disease were studied. Informed consent was obtained from the patients or their parents, as well as from control subjects.

The patients' clinical features were assessed by careful review of their medical records. Pathological features of all patients were independently evaluated by four authors (S.W., M.C.V.M., I.N. and I.N.). All patients have undergone a battery of histochemical stains, including haematoxylin and eosin, modified Gomori–trichrome (mGT), NADH-tetrazolium reductase (NADH-TR) and myosin ATPase.

In order to evaluate the genotype–phenotype correlation in CCD patients, the patients were divided into four groups, respectively, provided that they had one heterozygous C-terminal mutation, one heterozygous non-C-terminal mutation, two heterozygous mutations or no mutation.

Data were entered in Statistics Software for Social Sciences (SPSS version 11.0). Demographic characteristics were analysed by computation of the frequency, the mean ± standard deviation (SD), or the mean ± standard error of means (SEM), whichever was appropriate. The data then were subjected to a univariate analysis (Fisher's exact test). For comparing age and type 2 fibre deficiency, Mann–Whitney test was employed.

Mutational analysis

Genomic DNA was extracted from either muscle biopsy samples or peripheral blood lymphocytes according to standard protocols (Sambrook *et al.*, 2001). PCR primers were designed to amplify all 106 exons of *RYR1*, all five exons of *FKBP12* and the seven

exons of *CACNA1S* (exon 14–17 and 25–27) that encode the RYR1-interacting region (Peng *et al.*, 1998). Amplified fragments were directly sequenced using BigDye Terminator® v3.1 Cycle Sequencing kits on ABI3100 automated Genetic Analyzer (Applied Biosystems™, USA). DNA sequences were analysed with the SeqScape program and compared with the reference genomic sequence of: *RYR1* (Genbank J05200), *FKBP12* (Genbank M92423) and *CACNA1S* (Genbank L33798).

Results

Patients

A total of 27 unrelated Japanese CCD patients were selected for the study, consisting of 7 males and 20 females (Table 1) ranging in age from 2 to 63 years [29 ± 19 years (mean ± SD)] at the time of muscle biopsy. DNA from the parents of two patients (Patients 23 and 25) were also studied.

Patients 1–8 underwent muscle biopsy because they had pertinent family history of MH and were considered to be MH susceptible. In Japan, the diagnosis of MH susceptibility is achieved by detecting enhancement in the rate of calcium-induced calcium release (CICR) from the sarcoplasmic reticulum in chemically skinned muscle fibres (Ibarra *et al.*, 2005), reflecting the underlying pathomechanism of this disorder, that is, a lower activation threshold of the SR calcium-release channel. Cores were incidentally found in the muscle biopsies of Patients 1–8; thus a working diagnosis of CCD was made despite the absence of any muscle symptoms in most of these patients. CICR rate was enhanced in all eight patients. There was no description about the MH susceptibility status on the medical records of other subjects (Patients 9–27).

Nemaline bodies were identified in Patients 11, 12 and 23 on mGT stain; hence they were labelled as having core/rod disease (CRD).

Mutations

A total of 23 different missense mutations affecting 19 residues in *RYR1* were identified, consisting of 3 previously reported and 20 newly identified missense mutations in 93% of CCD patients (Tables 1 and 2). Two patients did not have any mutation in *RYR1*. All mutations were heterozygous single nucleotide changes, except for the substitution of two consecutive nucleotides (c.14761_14762TT>AC) in Patient 21, which was predicted to result in a single amino acid change (p.F4921T). There were two common heterozygous *RYR1* mutations in this cohort: c.14581C>T (p.R4861C) and c.7522C>G (p.R2508C), identified in 4 out of 25 (16%) and in 3 out of 25 (12%) patients, respectively. No mutations were found in either *FKBP12* or *CACNA1S*.

Twenty-two of 25 (88%) had only one heterozygous mutation: 14 (56%) with a heterozygous C-terminal mutation and 8 (32%) with a heterozygous non-C-terminal mutation. The remaining three (12%) patients had two heterozygous mutations (Patients 23, 24 and 25). Only the parents of Patients 23 and 25 were screened for the respective pair of mutations, as samples were not available from the parents of Patient 24. In Patient 23, the mutation p.D60N was identified in exon 3 of her maternal allele while p.L3606P was found in exon 73 of her paternal allele. In Patient 25, p.E512K in exon 14 was inherited from her mother while p.R4893P in exon 102 was acquired from her father. No muscle samples were available for histological studies from the parents of these two patients. *RYR1* mutations were found in patients with CRD (Patients 11, 12 and 23) (Table 1, Fig. 1). None of the newly identified missense mutations were found in 300 control chromosomes. Eighteen of 19 amino acids predicted to be changed were highly conserved through *RYR1* evolution and most of them were also conserved across the *RYR* species, *RYR1*, *RYR2* and *RYR3* (Table 2).

The mutations found in this cohort of CCD patients are shown in Fig. 2 at their respective location in the *RYR1*, along with those reported previously. In this study, 6 mutations were located outside the mutational 'hot spots', 4 in N-terminal 'hot spot' and 13 in the C-terminal region. These mutations were carried by 8 out of 25 (32%), 4 out of 25 (16%) and 16 out of 25 (59%) patients, respectively. We did not find any mutation in the central 'hot spot' or domain 2 in our cohort.

Genotype–phenotype correlation

Among eight patients with a heterozygous non-C-terminal mutation, two showed mild limb muscle weakness while the others were asymptomatic. The exact age of onset was difficult to ascertain because of the paucity of symptoms. Significant clinical findings during pregnancy and birth were not reported in this group. On muscle histochemistry, type 2 fibre deficiency was seen in only one patient, as he had <1% of type 2 fibres, while these were >12% in others [37 ± 4% (mean ± SD)]. Minimal endomysial fibrosis was found in three patients (37%), while the others had no increase in the interstitial fibrous tissue.

In contrast, limb muscle weakness was present in all patients with C-terminal mutations, and significant symptoms were manifested during the perinatal period (Table 1). There was statistically significant association between the presence of mutation in the C-terminal domain and clinical phenotypic characteristic in the following categories: limb muscle weakness, poor foetal movement during pregnancy, presence of joint dislocation and delayed motor milestone (Fig. 3A). Endomysial fibrosis and type 2 fibre deficiency were observed in most, if not all, patients with C-terminal mutations (Fig. 3B).

In terms of core structure, most patients had single cores (95% of fibres), but multiple cores were also seen especially in patients with heterozygous non-C-terminal mutations. In mutations outside domain 3, most cores were located in the periphery or subsarcolemmal areas (71%). In patients with C-terminal mutations, cores were noted to be

Table 1 Summary of clinical and pathological features of the patients and *RYR1* mutations

Patient	Sex	Pregnancy and birth symptoms	Family history	Onset	Clinical symptoms					CICR	Type 2 fibres†	Type 1 fibres with cores†	Features of cores§					Nemaline bodies	Endomysial fibrosis	RYR1 mutations (Exon)
					Delayed motor milestone	Muscle weakness	Skeletal and/or articular malformation	Others	Age at biopsy (years)				Central cores	Rimmed' cores	Atypical cores	Single core	Multiple cores			
1	F	N	Yes	Ad	No	No	JC		25	E	32	93	15	39	20	83	17	No	Minimal	c.1422G>T, p.Q474H (13)*
2	F	N	Yes	Ad	No	D	Sc	Ptosis	37	E	27	93	22	9	12	96	4	No	No	c.7522C>T, p.R2508C (47)*
3	F	N	No	Ad	No	No			63	E	13	89	22	17	4	92	8	No	No	c.7522C>T, p.R2508C (47)*
4	F	N	No	Ad	No	No	Sc		35	E	13	84	14	11	14	84	16	No	No	c.7522C>T, p.R2508C (47)*
5	F	N	Yes	Ch	No	No	Sc		9	E	40	98	74	12	5	96	4	No	No	c.7522C>G, p.R2508G (47)*
6	M	N	Yes	Ad	No	No			34	E	65	78	14	39	10	86	14	No	No	c.7523G>A, p.R2508H (47)*
7	F	N	No	Ch	No	P			8	E	<1	39	28	9	12	89	11	No	Minimal	c.7635G>C, p.E2545D (48)*
8	M	N	Yes	Ad	No	No			48	E	75	24	43	8	27	99	1	No	Minimal	c.10100A>G, p.K3367R (67)*
9	F	N	No	Ch	Yes	P			4	ND	<1	99	34	75	1	>99	1	No	Moderate	**c.13703T>C, p.L4568P (94)***
10	F	PFM, FI, RI, PS	No	Bi	Yes	P	JD, JC		3	ND	1	99	78	62	1	100	0	No	Marked	**c.13891T>A, p.Y4631N (95)***
11	M	FI	No	In	Yes	G	JD, JC		3	ND	2	68	41	71	28	100	0	Yes	Moderate	**c.13900G>A, p.E4634K (95)***
12	F	PFM, FI	Yes	Bi	Yes	G	JD, JC		2	ND	1	98	12	88	1	100	0	Yes	Minimal	**c.13912G>A, p.G4638S (95)***
13	F	PFM	No	Ch	Yes	P	JC, Sc	FMI, HAP	3	ND	<1	86	80	70	13	98	2	No	Marked	**c.14572A>G, p.N4858D (101)***
14	F	FI	No	In	No	G	JD, JC, Sc		10	ND	1	99	81	74	15	99	1	No	Marked	**c.14581C>T, p.R4861C (101)**
15	M	N	No	Ch	Yes	P			10	ND	<1	99	86	80	1	>98	2	No	Minimal	**c.14581C>T, p.R4861C (101)**

16	F	RI, PS	No	Bi	Yes	P	JD, JC, Sc, Lo		2	ND	3	60	69	78	3	98	2	No	Marked	**c.14581C>T, p.R4861C (101)**
17	F	PFM	No	Ch	Yes	G	JD, Sc		2	ND	<1	98	58	76	5	99	1	No	Marked	**c.14581C>T, p.R4861C (101)**
18	M	N	No	Ch	Yes	P	JC, Lo		3	ND	<1	99	67	80	2	99	1	No	Minimal	**c.14582G>A, p.R4861H (101)**
19	F	PFM, FI, RI	No	Bi	Yes	G	JD, Sc	FMI	2	ND	<1	83	21	55	36	100	0	No	Minimal	**c.14693T>C, p.I4898T (102)***
20	F	PFM, FI	No	Ch	Yes	P			9	ND	<1	96	97	72	4	99	1	No	Minimal	**c.14759C>A, p.T4920N (102)***
21	M	N	Yes	Ch	No	P	Lo		6	ND	<1	>99	74	86	6	99	1	No	Minimal	**c.14761_14762TT>AC, p.F4921T (102)***
22	M	PFM, FI, RI	No	Bi	Yes	P	JD, Sc	FMI	3	ND	<1	99	34	82	23	82	18	No	Marked	c.14762T>C, p.F4921S (102)*
23	F	FI	Yes	In	Yes	P	Lo		5	ND	9	66	12	12	30	98	2	Yes	Moderate	c.178G>A, p.D60N (3); c.10817T>C, p.L3606P (73)*
24	F	FI, RI, PS	No	Bi	Yes	G	JD, Lo		10	ND	<1	14	58	62	9	99	1	No	No	c.1280C>T, p.S427L (13); **c.14696G>A, p.G4899E (102)***
25	F	FI, RI, PS	No	Bi	Yes	P	JD, Lo		2	ND	21	>99	89	66	29	98	2	No	Moderate	c.1534G>A, p.E512K (14); **c.14678G>C, p.R4893P (102)***
26	F	N	Yes	Ch	Yes	P	Sc		36	ND	13	99	94	0	74¶	98	2	No	Minimal	Not detected
27	F	N	No	Ad	No	D			35	ND	72	52	60	18	31	100	0	No	None	Not detected

C-terminal mutations are written in bold letters. F = female; M = male; N = normal; Ad = adolescence; Ch = childhood; Bi = birth; In = infancy; PFM = poor foetal movement; FI = floppy infant; RI = respiratory insufficiency; PS = poor sucking; JC = joint contracture, JD = joint dislocation; Sc = scoliosis; Lo = lordosis; FMI = facial muscle involvement; HAP = high-arched palate; D = distal, P = proximal, G = generalized; CICR = calcium-induced calcium release; E = enhanced; ND = not done. * Novel mutations; §Values expressed as percentage of cores; †Values expressed as percentage of fibres; ¶Refer to text and/or figure for description of cores.

Table 2 Comparison of amino acid in the affected residues with that from mouse, pig, rabbit and other human RYR proteins, RYR2 and RYR3

Residue	60	427	474	512	2508	2545	3367	3606	4568	4631	4634	4638	4858	4861	4893	4898	4899	4920	4921
Predicted change	N*	L*	H*	K*	G/H/C*	D*	R*	P*	P*	N*	K*	S*	D*	H/C	P*	T	E*	N*	S/T*
RyR1																			
Human	D	S	Q	E	R	E	K	L	L	Y	E	G	N	R	R	I	G	T	F
Mouse	D	S	Q	E	R	E	K	L	L	Y	E	G	N	R	R	I	G	T	F
Pig	D	S	Q	E	R	E	K	L	L	Y	E	G	N	R	R	I	G	T	F
Rabbit	D	S	Q	E	R	E	K	–	L	Y	E	G	N	R	R	I	G	T	F
RyR2																			
Human	D	K	Q	E	R	D	K	L	L	Y	E	G	N	R	R	I	G	T	F
RyR3																			
Human	D	–	Q	M	R	E	K	V	L	Y	Q	G	N	R	R	I	G	T	F

*Novel mutations.

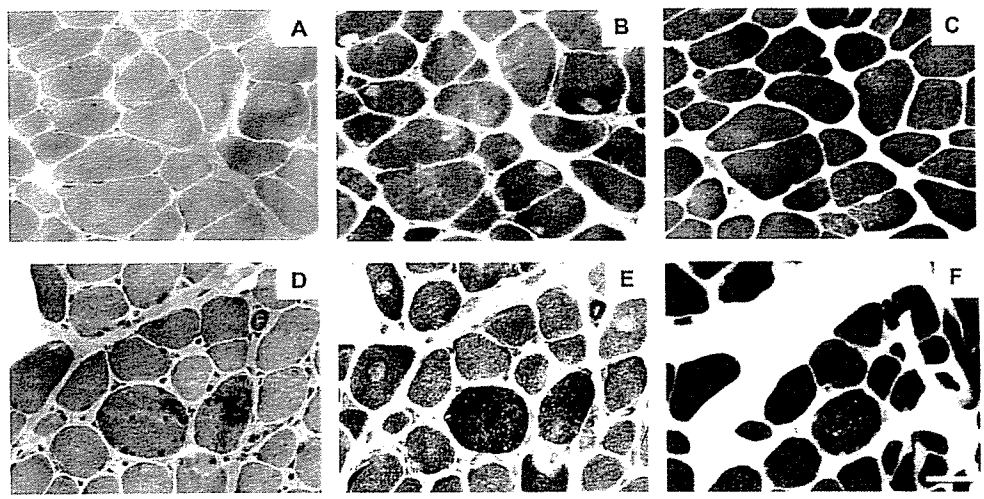

Fig. 1 Muscle biopsy. (**A–C**) A 10-year-old patient with a double mutation. (**A**) Minimal fibrosis is observed in mGT section. (**B**) NADH shows cores in type 1 fibres. (**C**) ATPase staining at pH 4.6 shows type 2 fibre deficiency. (**D–F**) A 3-year-old with nemaline bodies in muscle fibres. (**C**) Nemaline bodies and moderate fibrosis are depicted in mGT section. (**D**) Fibres with nemaline bodies have high enzymatic activity; typical central cores are noted. (**E**) ATPase staining with pH 4.3 pre-incubation demonstrates type 2 fibre deficiency. Bar denotes 50 microns.

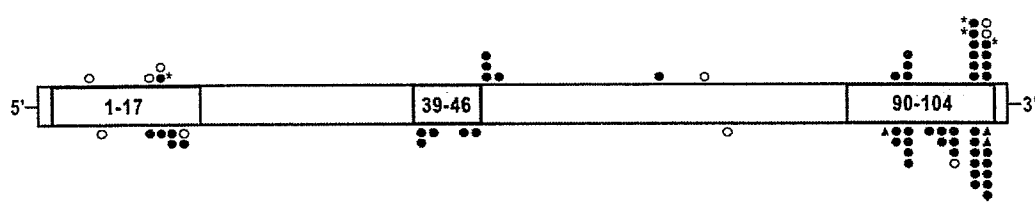

Fig. 2 *RYR1* mutation map for CCD. The three mutational hot spot areas are shaded: CCD domain 1: 1–17; CCD domain 2: 39–46; CCD domain 3: 90–104. Missense mutations (closed circle) found in this study are shown at the top; previously reported mutations are indicated at the bottom. Open circle: recessive mutation; triangle: deletions; asterisk: mutations identified in this study but were also included in previous reports.

characteristic: these were ovoid in shape and with clearly demarcated borders, and were predominantly located in the centre of the fibres [60 ± 7% (mean ± SEM)]; they also occurred singly (98 ± 4%). In addition, most of the cores (72 ± 5%) in this group appeared to be 'rimmed' (Fig. 4B), which may connote high enzymatic activities around the cores on NADH-TR stain. More cores in type 1 fibres were also noted (90 ± 4%), but in general the percentage of the fibres with cores varied from 3 to 100%. No correlation was seen between clinical severity and the percentage of cores in fibres.

Some fibres show 'atypical' cores, characterized by indistinct borders and whose shapes were inexplicitly ovoid (Fig. 4E). These were seen more in non-C-terminal mutations but no statistical significance was observed as compared with C-terminal mutations (Fig. 3B). Like in typical core structures, these were also noted to be either in the centre of the fibre or in the subsarcolemmal areas.

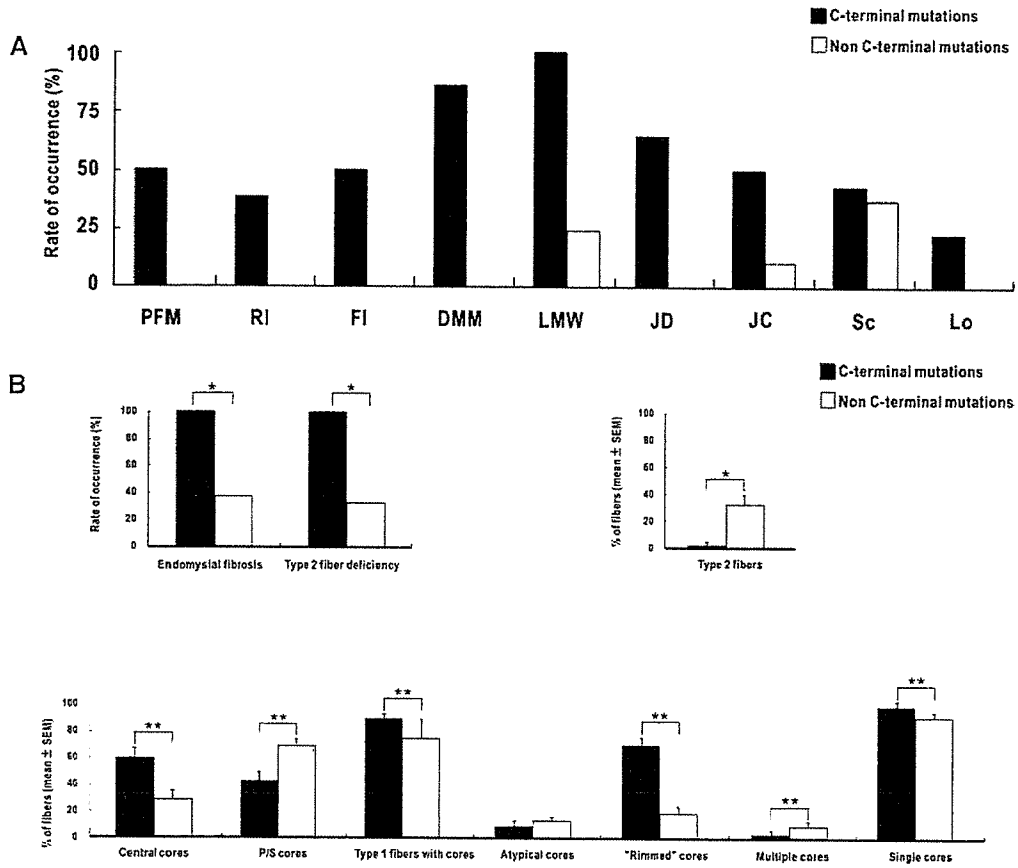

Fig. 3 (**A**) Genotype–phenotype correlation (clinical). Comparison of the clinical features between the patients with a heterozygous C-terminal mutation and those with a heterozygous non-C-terminal mutation. PFM = poor foetal movement; RI = respiratory insufficiency; FI = floppy infant; DMM = delayed motor milestone; JD = joint dislocation; JC = joint contracture; S = scoliosis; L = lordosis; LMW = limb muscle weakness. *$P < 0.05$, Fisher's exact test. (**B**) Genotype–phenotype correlation (pathological). Comparison of the pathological features between the patients with a heterozygous C-terminal mutation and those with a heterozygous non-C-terminal mutation. Note the characteristic endomysial fibrosis and fibre type 2 deficiency in patients with C-terminal mutations (upper panel). P/S = peripheral or subsarcolemmal. *$P < 0.05$, Fisher's exact test. **$P < 0.05$, Mann–Whitney test; SEM, standard error of means.

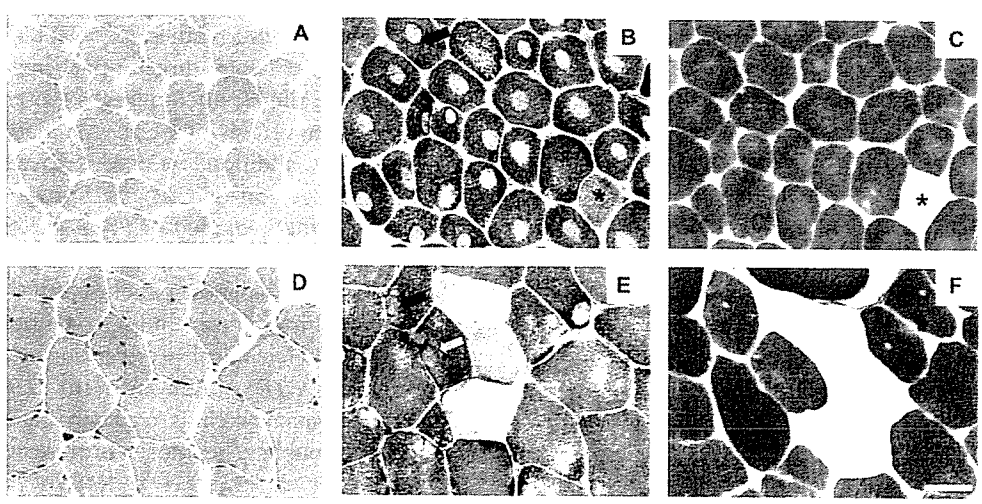

Fig. 4 Muscle biopsy. (**A–C**) A 9-year-old patient with a mutation in C-terminal region. (**A**) Minimal fibrosis is seen in mGT. (**B**) NADH-TR stain reveals the 'central core' in almost all fibres; note the 'rimming' of some cores (arrow). (**C**) Myosin ATPase staining, pH 4.4, clearly demonstrates type 2 fibre deficiency; type 2 fibre is marked with asterisk. (**D–F**) A 63-year-old patient with non-C-terminal mutation. (**D**) Minimal fibrosis is observed in mGT. (**E**) NADH shows cores but not on all type I fibres; note atypical cores (red arrow) and multiple cores in fibres (yellow arrow). (**F**) ATPase at pH 4.5 shows type 2 fibres in higher frequency compared with patient with C-terminal mutation. Bar denotes 50 microns.

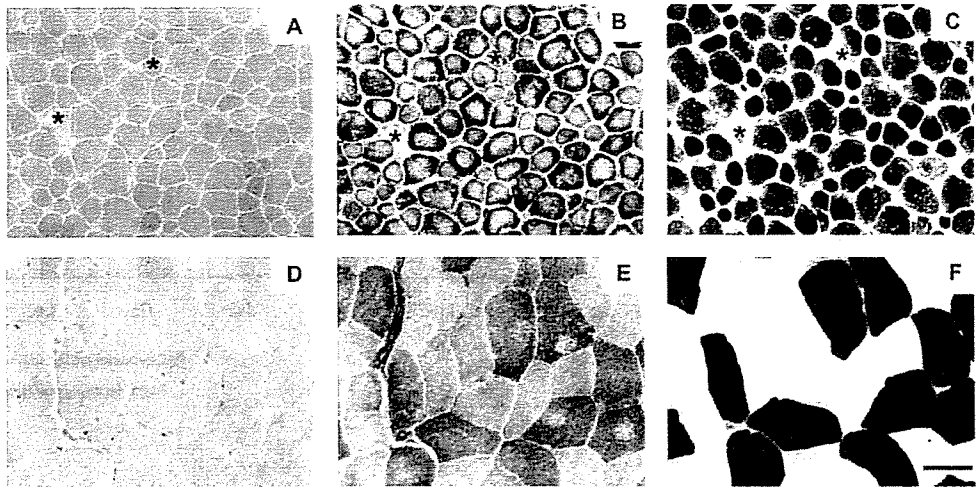

Fig. 5 Sections from patients in whom mutations were not found. (**A–C**) Sections from a 36-year-old female. (**A**) Moderate endomysial fibrosis is observed in mGT. (**B**) Cores are seen in almost all fibres; note that cores occupy the whole diameter of fibres, and the subsarcolemmal area surrounding the cores has high oxidative enzyme activity. (**C**) Type 2 fibre (asterisk) deficiency is seen in ATPase with pH 4.4 pre-incubation. (**A–C**) Biopsy findings from a 35-year-old female. (**D**) No endomysial fibrosis is noted in mGT. (**E**) Cores were seen but only in few type 1 fibres. (**F**) No fibre type 2 deficiency is observed (type 2 fibres comprised 72%). (**C**) Scale bar denotes 50 microns.

In Patients 1–8, from whom muscle biopsy was performed for CICR and cores were incidentally identified, all had non-C-terminal heterozygous mutations.

The clinical features of patients with two heterozygous mutations were more similar to those of the group with one heterozygous C-terminal mutation. In terms of muscle pathology, type 2 fibre deficiency was likewise seen (Table 2), similar to mutations involving the C-terminal region. This idea may also be buttressed by the fact that among a total of three patients with CRD, two carried a single C-terminal mutation, while the other had a compound heterozygous mutation. In terms of core pathology, however, they resemble that of non-C-terminal mutations: the cores were seen in 14 and 49% of type 1 fibres in Patients 24 and 25, respectively; and the characteristic 'rimming' of cores is less appreciated (Fig. 1).

In two patients in whom no mutation was found, the cores had peculiar features distinguishable from that seen in patients with identifiable mutations. Particularly, in Patient 26, the cores, albeit located centrally, occupied almost the whole diameter of the fibre, and, notably, the subsarcolemmal area around the cores had increased oxidative activity (Fig. 5). The cores in Patient 27 were initially considered to be regular cores but a closer look has shown that almost all the cores had indistinct borders; moreover, only <20% of type 1 fibres have cores (Fig. 5). In such cases, the term 'core-like' may be more appropriate to describe these structures.

Discussion

RYR1 mutations in CCD

At least 44 reported *RYR1* mutations have been associated with CCD, including 39 missense mutations and 5 deletions (Quane *et al.*, 1993; Zhang *et al.*, 1993; Fletcher *et al.*, 1995; Manning *et al.*, 1998; Lynch *et al.*, 1999; Monnier *et al.*, 2000, 2001; Avila and Dirksen, 2001; Tilgen *et al.*, 2001; Ferreiro *et al.*, 2002; Jungbluth *et al.*, 2002; Robinson *et al.*, 2002; Sewry *et al.*, 2002; Avila *et al.*, 2003*a*; Quinlivan *et al.*, 2003; Zorzato *et al.*, 2003; Shepherd *et al.*, 2004). All these mutations are clustered in the three 'hot spots', except for two (Fig. 2). *RYR1* mutations have been reported to be responsible for 47–67% of patients suffering from CCD, implying that the disease is genetically heterogeneous (Vainzof *et al.*, 2000; Monnier *et al.*, 2001). However, neither the true frequency nor the distribution of CCD-causative mutations has been accurately determined to date, since mutation screening has been limited to the three 'hot spots' of the *RYR1*, or even only to the C-terminal region. According to *in vitro* studies, two RYR1-binding proteins, *FKBP12* and *CACNA1S*, directly participate in or modulate EC coupling, while EC uncoupling is thought to be the linchpin in the pathogenesis of CCD (Avila *et al.*, 2001; Lyfenko *et al.*, 2004). In addition, mutations have been identified in RYR1-binding region of *CACNA1S* in 1% of patients with MH. We therefore regarded *FKBP12* and *CACNA1S* genes as rational candidates for CCD.

We screened 27 Japanese patients with CCD, diagnosed on the basis of histological findings, without putting much emphasis on their clinical presentation as inclusion criteria, and found that *RYR1* mutations occur in 93% (25 out of 27) of CCD patients, which is a much higher rate than that thought previously. The most common CCD mutation in our cohort was c.14581C>T (p.R4861C). Interestingly, the c.14582G>A (p.R4861H) mutation that affects the same amino acid is the most common CCD mutation in European countries, while it was identified in only one patient from our series. Almost all reported patients bearing c.14582G>A had a positive family history, but all patients carrying mutation c.14581C>T were sporadic in this study and also in the

literature (Monnier *et al.*, 2001; Tilgen *et al.*, 2001; Davis *et al.*, 2003), suggesting that the 14 581 nucleotide might be susceptible to change.

To our knowledge, this is the first endeavour to screen the entire coding region of *RYR1* in a cohort of CCD patients. By screening the C-terminal region alone, we would have found *RYR1* mutations only in 59% (16 out of 27) of CCD patients, which is consistent with detection rates in previous reports, missing the two compound heterozygous mutations. Even extending the mutation screening to the three 'hot spots', we would have found *RYR1* mutations in only 67% (18 out of 27), also missing one compound heterozygous mutation. It thus becomes necessary to screen the entire *RYR1* coding region in CCD patients, however impractical it may be owing to the size of the gene. Interestingly, most of mutations outside the 'hot spots' were localized in exons 47 and 48, which neighbour the central region 'hot spot' (exons 39–46). Hence, mutation detection rate in CCD patients could be increased up to 89% by including exons 47 and 48, which may be a more practical alternative than sequencing the entire *RYR1* gene. In addition, *FKBP12* and *CACNA1S* may not be causative genes for CCD or an extremely rare, if they are, since there was no mutation in *FKBP12* or in the RYR1-binding region of *CACNA1S* genes.

We did not find any mutation in two patients in our cohort, suggesting that CCD may still be genetically heterogeneous even though there still remains the possibility that mutations may exist in unexamined regions, such as promoter region and introns, or that we may have overlooked a mutation. Notwithstanding this likelihood of other probabilities, the pathological characteristics of these patients are clearly different from the rest. If these patients were excluded from the analysis solely on the basis of the 'uncharacteristic' core-like structures, that is, if the inclusion criteria used were more stringent, the detection rate of mutations involving the *RYR1* gene will considerably and significantly increase to 100%.

Probable autosomal recessive CCD

CCD was once thought to be inherited solely via an autosomal dominant mechanism, but actually rare instances of recessive inheritance have also been identified (Manzur *et al.*, 1998; Ferreiro *et al.*, 2002; Romero *et al.*, 2003).

In this study, sequencing of the entire *RYR1* coding regions led to the identification of three patients (Patients 23, 24 and 25) with two heterozygous mutations. Patients 24 and 25 needed respiratory mechanical assistance after delivery, while their parents were completely healthy and without any skeletal abnormalities. In both patients, each of the two heterozygous mutations was, respectively, found in each of the parents, confirming that these patients had a compound heterozygous mutation. In Patient 25, p.R4893P affected the third residue of a very well conserved GVRAGGGIGD luminal motif (amino acids p.G4891-D4900) that has been proposed to be a pore-forming fragment responsible for the electrophysiological characteristics of the channel (Zhao *et al.*, 1999).

The parents of Patients 23 and 25 were asymptomatic, while they had heterozygous mutation, suggesting the recessive nature of these mutations. Since CCD patients could be clinically asymptomatic, however, we may not be able to completely exclude the possibility that their parents could have CCD. Nevertheless, judging from the clinical features and the mutation data, autosomal recessive mode of inheritance is most likely in these particular patients. Patient 24 also carried two heterozygous mutations (p.S427L in exon13, p.G4899E in exon 102), but further analysis was inevitably limited by the unavailability of samples from her parents, hampering full evaluation if this was indeed an autosomal recessive case. The p.G4899E mutation also affected the very well conserved GVRAGGGIGD luminal motif (G4899 underlined). Interestingly, this mutation has been reported in two papers as a causative heterozygous mutation (Monnier *et al.*, 2001; Romero *et al.*, 2003); however, since only the 'hot spots' were screened in these studies, the presence of another mutation is still possible and hence it might be impetuous to conclude that p.G4899E mutation is a causative dominant mutation.

Genotype–phenotype correlation

In general, CCD has a wide spectrum of phenotypic expression, ranging from the apparent absence of symptoms to the presence of perinatal complications and generalized muscle weakness. Mutations in the C-terminal region seem to be associated with certain clinical and pathological features: hypotonia during infancy, delayed motor development and limb muscle weakness; type 2 fibre deficiency and interstitial fibrosis; and characteristic cores with clearly demarcated borders, which are observed in almost all type 1 muscle fibres. In addition, 'rimming' on the borders of these cores is observed in much higher frequency; similarly, this phenomenon was also noted in the biopsy specimens of three families determined to have mutation in domain 3 (Sewry *et al.*, 2002). These unique features therefore delineate C-terminal mutations from other groups, at least in terms of muscle pathology.

In contrast, most of CCD patients harbouring at least one mutation outside the C-terminal region had only mild musculoskeletal abnormalities such as joint contractures and scoliosis. This phenomenon may be explained by the leaky-channel model and EC uncoupling model. Some non-C-terminal mutations in *RYR1* promote the leak of Ca^{2+} ions from the SR that may or may not be compensated by the activity of the sarco-endoplasmic reticulum Ca^{2+} ATPase (SERCA), resulting in an elevation of resting cytosolic Ca^{2+} and a depletion of SR Ca^{2+} stores. On the other hand, C-terminal mutations, especially those in the pore region of *RYR1*, may directly affect the channel gating properties, resulting in an abolition of orthograde activation by the